Electronic Supplementary Information

Sustainable Aviation Fuel from Prehydrolysis Liquors

Daria Lebedeva,[a] Lars William Schick,[a] Withsakorn Sangsuwan,[a] Gonzalo Castiella-Ona,[a] Dagoberto O. Silva,[c] Daniel Cracco,[a] Alessandro Marson,[d] Erik Svensson Grape,[b] A. Ken Inge,*[b] Liane M. Rossi,*[c] Alessandro Manzardo,*[d] Elena Subbotina*[a] and Joseph S. M. Samec*[a]

[a] Stockholm University, Department of Organic Chemistry, Svante Arrhenius väg 16C, SE 106 91 Stochholm, Sweden

E-mail: joseph.samec@su.se

[b] Department of Materials and Environmental Chemistry, Stockholm University, Stockholm SE-10691, Sweden

[c] Departamento de Química Fundamental, Instituto de Química, Universidade de São Paulo, Av. Prof. Lineu Prestes, 748, 05508-000, São Paulo, SP, Brazil

[d] CESQA (Quality and Environmental Research Center), University of Padova, Department of Civil, Environmental and Architectural Engineering, Via Marzolo 9, 35131 Padova, Italy

Contents

Determination of carbohydrate and lignin content in wood

A two-step hydrolysis procedure (NREL/TP-510-42618):

Sawdust sample (0.3 g) and H_2SO_4 (3 mL, 72 wt% aq. solution) were added to a sealed pressure tube and stirred for 1 h at 30 °C. The resulting mixture was diluted with DI water (84 mL) and stirred for additional an additional hour at 120 °C. The mixture was then cooled to room temperature and filtered to separate the liquid from the solid residue. An aliquot of the filtrate was neutralized by adding $CaCO_3$ to achieve a pH of 6-7, and subjected to HPLC. The solid residue was washed with DI water, dried overnight, weighted, and then incinerated at 575 °C to determine the ash content. The weight difference obtained after incineration represents the acid-insoluble lignin (AIL) content.

The compositions of both the initial raw material and the pre-treated material are presented in Table S1.

Table S1. Composition of birch sawdust.

Biomass component	Content in raw material, wt%	Content in pre-treated sample, wt%
Xylan	25	1
Glucan	32	55
Lignin (AIL)	19	31

Determination of monosaccharides in pre-hydrolysis liquor

Prehydrolysis liquor was analyzed by HPLC. Monosaccharides were quantified using calibrated samples. The composition of the prehydrolysis liquor is shown in Table S2.

Table S2. Monosaccharide composition of pre-hydrolysis liquor.

Monosaccharide	Content, wt.% based on wood raw material
Xylose	8.1
Glucose	0.4
Galactose	1.0
Arabinose+Mannose	3.1

Dehydration of xylose

Reaction optimization

The optimization of temperature and reaction time was carried out. It was observed that the furfural yield increased with rising temperature. Reactions conducted at 100 °C, 140 °C, and 180 °C yielded 14%, 46%, and 65%, respectively (Table S3, Entries 2-4). A higher temperature led to lower yields (Table S3, Entry 5), probably due to humin formation as a result of undesired furfural condensation at higher temperatures. Additionally, it was also noted that if the reaction time exceeded 1 h, the yield decreased (Table S3, Entry 6). On the other hand, shortening the reaction time to 30 min resulted in a yield to 62% (Table S3, Entry 7). An increase in yield was observed when water was used as an additive, with a furfural yield of 74% (Table S3, Entry 1). Increasing the H_2O/EtOAc ratio lowered the yield to 71% and 68% for 1:10 and 1:5 ratios, respectively (Table S3, Entries 8 and 9). It has been proposed that the role of water was to solubilize sugars and enhance their conversion.

Table S3. Dehydration of xylose.

Entry	T, °C	Time, h	H_2O/EtOAc	Yield, %
1	**180**	**1**	**1:20**	**74**
2	100	1	-	14
3	140	1	-	46
4	180	1	-	65
5	220	1	-	53
6	180	1.5	-	59
7	180	0.5	-	62
8	180	1	1:10	71
9	180	1	1:5	68

Determination of the furfural yield

Furfural yield was quantified by GC-FID using dodecane as an internal standard. The relative response factor (RRF) was calculated using effective carbon number (ECN) by the following equations:

(1) $$RRF_i = \frac{\mathrm{ECN}_i}{\mathrm{ECN}_{std}} \times \frac{\mathrm{M}_{std}}{\mathrm{M}_i} \quad ,$$

(2) $$m_i = \frac{\mathrm{A}_i}{\mathrm{A}_{std}} \times \frac{\mathrm{m}_{std}}{\mathrm{RRF}_i} \quad ,$$

where A_i and A_{std} are peak areas of identified compounds(*i*) and a standard (*std*), respectively, m – mass, M – molar mass.

Achmatowicz rearrangement optimization

Various solvents were tested for reaction optimization (Table S4, Entries 1-5). The highest selectivity for the targeted product was achieved when the reaction was conducted in 2-propanol (Table S4, Entry 5). The optimal reaction time was found to be 5 h (Table S4, Entry 5). Shortening the reaction time did not result in full conversion of the starting material (Table S4, Entry 6). On the other hand, extending the reaction time led to a decrease in selectivity (Table S4, Entries 7 and 8), probably due to the poor stability of the product under oxidizing conditions, as described in the main text. Maintaining the reaction at 0°C when adding the starting material was essential for achieving higher selectivity. The difference in selectivity between adding the material at 0°C and at room temperature was 63% and 37%, respectively (Table S4, Entries 9 and 10). Increasing the catalyst loading resulted in a lower yield (Table S4, Entry 11), likely due to the poor stability of the product, as described in the main text. Finally, by optimizing the quenching procedure, we were able to achieve an isolated yield of 98% in the Achmatowicz rearrangement.

Table S4. Achmatowicz reaction optimization. Standard reaction conditions for reaction optimization without work-up: MTO (12.5 mg, 50 µmol, 1 mol%) was combined with hydrogen peroxide (855.9 mL, 35%, 5 mmol) and cooled to 0 °C. The mixture was stirred for 15 min. A solution of furfuryl alcohol (490 mg, 5 mmol) in 2-propanol (2.6 mL) was added dropwise to the oxidation solution. The resulting mixture was stirred for 5 h, allowing the temperature to rise to r.t.

[1] Work-up procedure: Molecular sieves (1.5 g) were added, and the mixture was left to stir for an additional hour. The reaction mixture was then filtered through a celite plug, condensed under reduced pressure, and left to crystallize in the freezer overnight. The following morning, the precipitate was filtered off and dried under high vacuum, yielding a colourless crystalline solid. [2] Isolated yield.

Entry	Deviation from standard conditions	NMR yield, %	Selectivity, %	Conversion, %
1	MeOH	52	53	99
2	EtOH	63	72	88
3	*t*-BuOH	70	70	100
4	MeCN	16	16	100
5	-	85	85	100
6	2 h reaction	59	76	78
7	6 h reaction	73	73	100
8	2 d reaction	48	48	100
9	EtOH, 3h, addition at r.t	26	37	71
10	EtOH, 3h, addition at 0 °C.	63	63	100
11	$MeReO_3$ (2 mol%) 6.5 h, EtOH	52	52	100
12[1]	work-up using MS	98[2]	98	100

Absorption spectra of 6-methoxy-2H-pyran-3(6H)-one

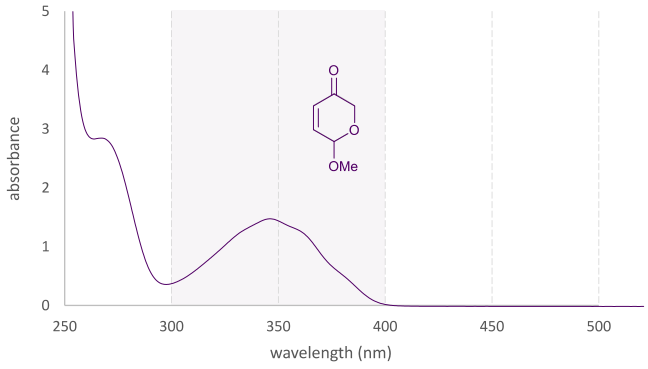

Figure S1. Absorption spectra of 6-methoxy-2H-pyran-3(6H)-one.

Absolute configuration of cycloadducts

The absolute configuration of isolated cycloadducts was established by single-crystal X-ray analysis (Figure S2-S4 and Table S5). Single crystal X-ray diffraction data on suitable crystals of cycloadducts 1, 2 and 3 were collected using Cu Kα radiation on a Bruker D8 VENTURE diffractometer equipped with a PHOTON 100 detector. The datasets were reduced and absorption correction was applied using the APEX3 suite. The crystal structures were solved and refined by SHELXT and SHELXL respectively.[1,2] The refinements were carried out using a full-matrix least-squares approach based on F^2 with all non-hydrogen atoms anisotropically defined. All hydrogen atoms could be located in the Fourier difference map. CCDC 2307840-2307841 and CCDC 2308513 contain the supplementary crystallographic data for

this paper. These data can be obtained free of charge from The Cambridge Crystallographic Data Center via http://www.ccdc.cam.ac.uk/structures.

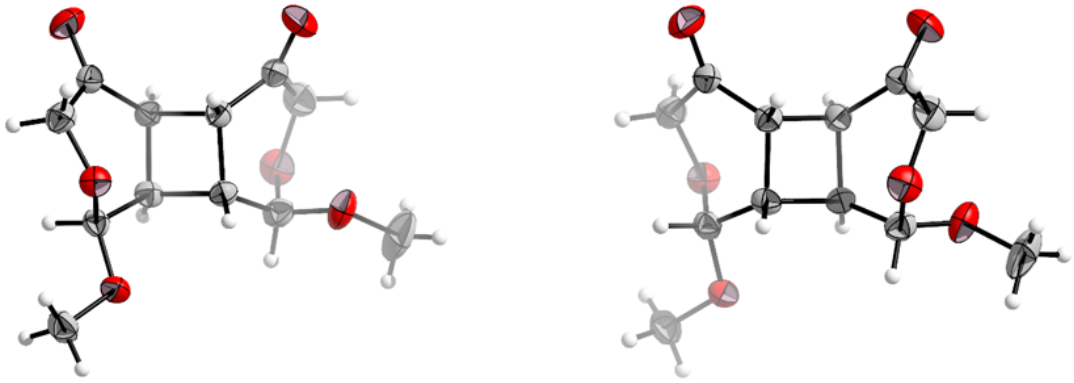

Figure S2. Absolute configuration of HH cycloadduct (cycloadduct 1 in the main text) as determined by single-crystal X-ray diffraction. Crystals contained a racemic mixture. Thermal ellipsoids are drawn at a 50 % probability level.

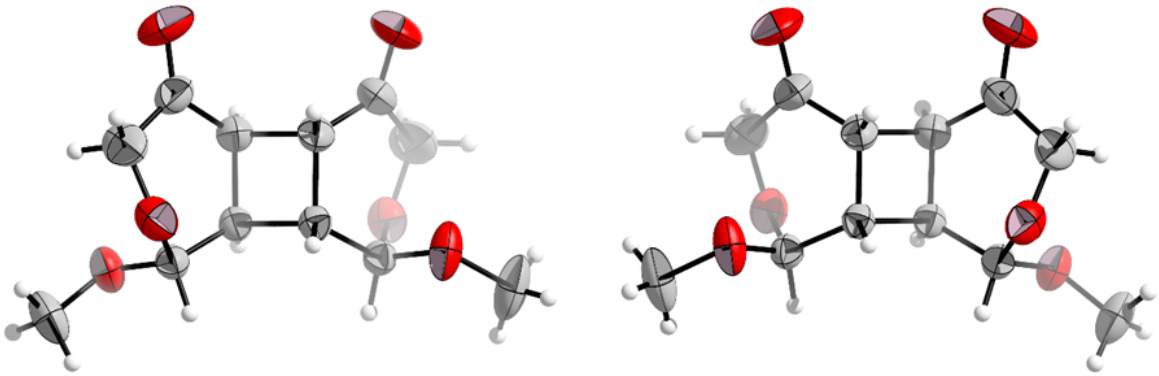

Figure S3. Absolute configuration of HH cycloadduct (cycloadduct 2 in the main text) as determined by single-crystal X-ray diffraction. Crystals contained a racemic mixture. Thermal ellipsoids are drawn at a 50 % probability level.

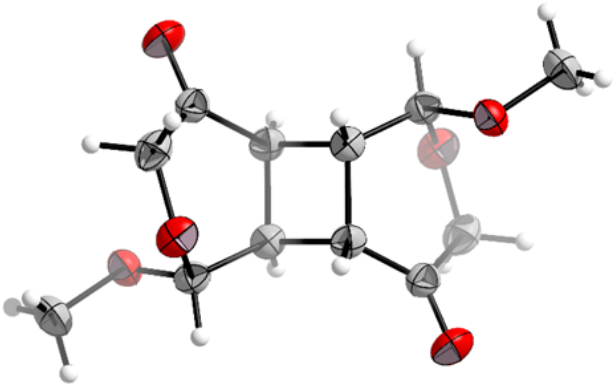

Figure S4. Absolute configuration of HT cycloadduct (cycloadduct 3 in the main text) as determined by single-crystal X-ray diffraction. Thermal ellipsoids are drawn at a 50 % probability level.

Table S5. Crystallographic data and refinement details for cycloadducts 1, 2 and 3.

	cycloadduct 1	**cycloadduct 2**	**cycloadduct 3**
Identification code	CCDC 2308513	CCDC 2307841	CCDC 2307840
Empirical formula	$C_{12}H_{16}O_6$	$C_{12}H_{16}O_6$	$C_{12}H_{16}O_6$
Formula weight	256.25 g mol^{-1}	256.25 g mol^{-1}	256.25 g mol^{-1}
Temperature	294(2) K	294(2) K	294(2) K
Wavelength	1.54178 Å	1.54178 Å	1.54178 Å
Crystal system	Orthorhombic	Monoclinic	Monoclinic
Space group	*Pbca* (No. 61)	$P2_1/c$ (No. 14)	$P2_1/c$ (No. 14)
Unit cell dimensions	*a* = 10.5173(6) Å *b* = 8.6150(5) Å *c* = 26.809(1)Å	*a* = 9.4404(3) Å *b* = 14.2743(4) Å *c* = 9.8596(3) Å *β* = 111.083(1)°	*a* = 7.1937(2) Å *b* = 9.3874(3) Å *c* = 8.8093(3)Å *β* = 98.709(1)°
Volume	2429.1(2) $Å^3$	1239.69(7) $Å^3$	588.03(3) $Å^3$
Z	8	4	2
Density (calc.)	1.401 g cm^{-3}	1.373 g cm^{-3}	1.447 g cm^{-3}
Absorption coefficient	0.959 mm^{-1}	0.940 mm^{-1}	0.991 mm^{-1}
F(000)	1088	544	272
Crystal size	0.71 × 0.54 × 0.20 mm^3	0.54 × 0.56 × 0.62 mm^3	0.54 × 0.44 × 0.37 mm^3
ϑ range for data collection	3.297 to 70.109°	5.021 to 74.623°	6.224 to 67.679°
Index ranges	$-12 \le h \le 11$ $-10 \le k \le 10$ $-32 \le l \le 32$	$-11 \le h \le 11$ $-17 \le k \le 17$ $-12 \le l \le 12$	$-8 \le h \le 8$ $-11 \le k \le 11$ $-10 \le l \le 10$
Reflections collected	20488	30151	10018
Independent reflections	2314 [R(int) = 0.0637]	2552 [R(int) = 0.0397]	1155 [R(int) = 0.0467]
Absorption correction	Multi-scan	Multi-scan	Multi-scan
Min. and max. transmission	0.4177 and 0.7533	0.6099 and 0.7538	0.5193 and 0.7536
Data / restr. / param.	2314/0/196	2552/0/166	1155/0/106
Goodness-of-fit on F^2	1.048	0.936	1.075
Final R indices [I > 2σ(I)]	R1 = 0.0431, wR2 = 0.1121	R1 = 0.0430 wR2 = 0.1408	R1 = 0.0336 wR2 = 0.0828
Largest diff. peak and hole	0.341 and -0.197 e $Å^{-3}$	0.220 and -0.211 e $Å^{-3}$	0.166 and -0.168 e $Å^{-3}$

HDO of cycloadducts

Determination of the hydrocarbon yield

Due to the complexity of the product mixture, individual components were identified indirectly using the most reliable GC-MS/FID analysis. The mass spectra of the individual peaks support cyclobutane formation (see below). In addition, we analysed the resulting hydrocarbon mixture by GCxGC method, using the standard library for petroleum-based fuels and were not able to see standard petroleum-derived components, such as aromatics or linear alkanes, indirectly supporting the cyclobutane formation.

The yield of hydrocarbons was determined using GC-FID. Dodecane was utilized as an internal standard. The relative response factor (RRF) was calculated using effective carbon number (ECN) by the following equations:

(1) $$RRF_i = \frac{\mathrm{ECN}_i}{\mathrm{ECN}_{std}} \times \frac{\mathrm{M}_{std}}{\mathrm{M}_i} \quad ,$$

(2) $$m_i = \frac{\mathrm{A}_i}{\mathrm{A}_{std}} \times \frac{\mathrm{m}_{std}}{\mathrm{RRF}_i} \quad ,$$

Where A_i and A_{std} are peak areas of identified compounds(*i*) and a standard (*std*), respectively, m – mass, M – molar mass.

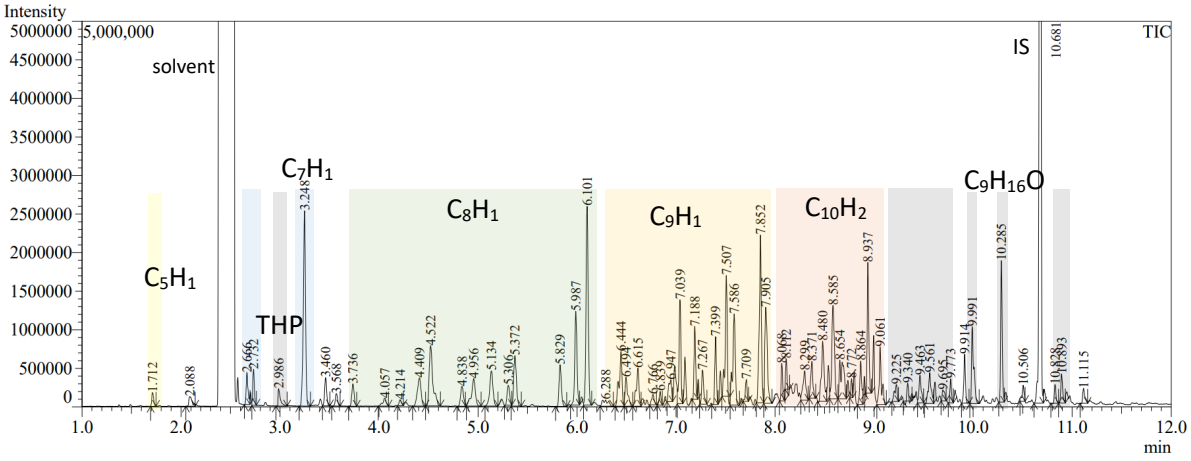

Figure S5. GC-Mass spectrum of the hydrocarbon mixture after HDO of cycloadducts (optimized conditions, Table 2, Entry 1, in the main text).

Mass fragmentation spectra of detected compounds

THP:

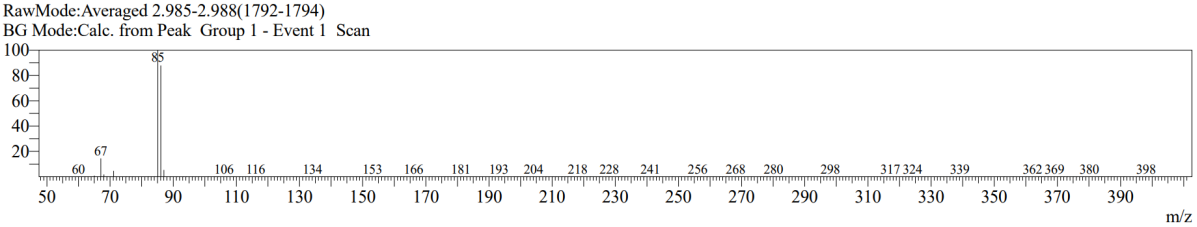

C_7H_{14}:

RawMode:Averaged 3.245-3.248(1948-1950)
BG Mode:Calc. from Peak Group 1 - Event 1 Scan

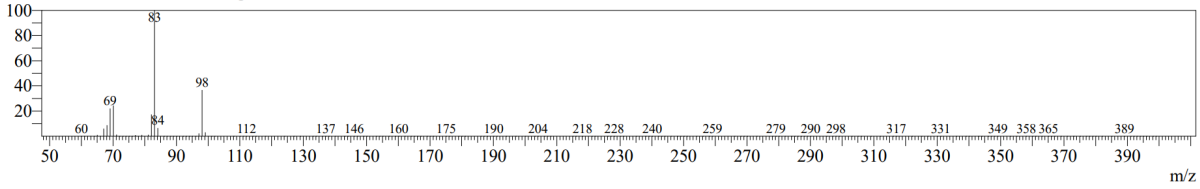

C_8H_{16}:

RawMode:Averaged 5.985-5.988(3592-3594)
BG Mode:Calc. from Peak Group 1 - Event 1 Scan

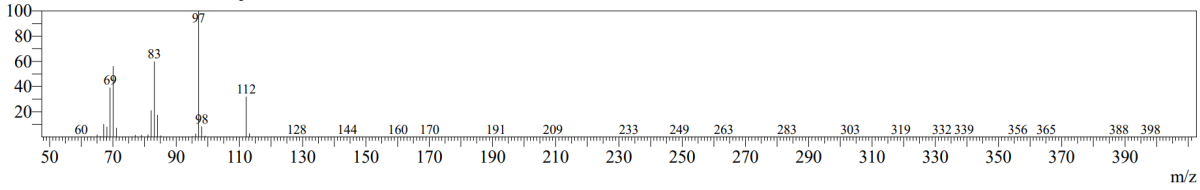

C_9H_{18}:

RawMode:Averaged 7.038-7.042(4224-4226)
BG Mode:Calc. from Peak Group 1 - Event 1 Scan

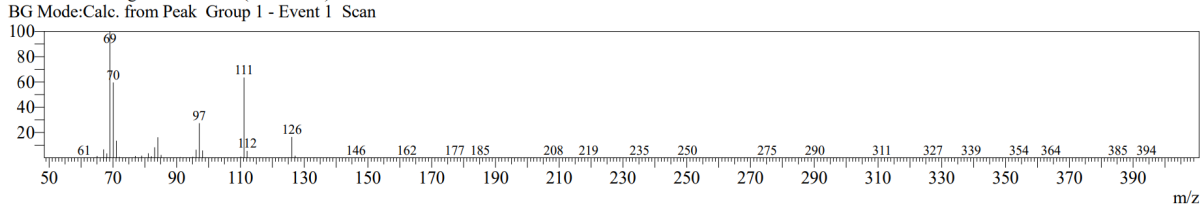

$C_{10}H_{20}$:

RawMode:Averaged 8.935-8.938(5362-5364)
BG Mode:Calc. from Peak Group 1 - Event 1 Scan

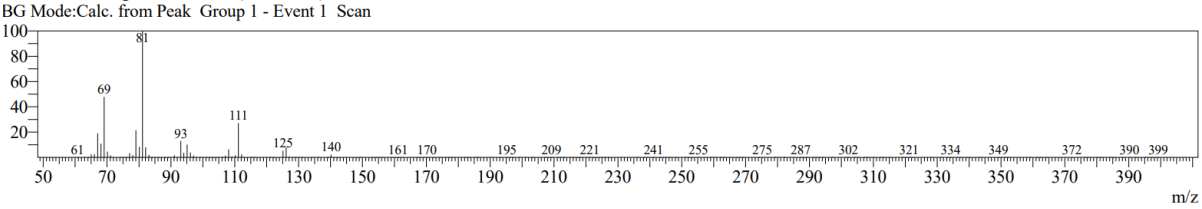

$C_9H_{16}O$:

RawMode:Averaged 10.283-10.287(6171-6173)
BG Mode:Calc. from Peak Group 1 - Event 1 Scan

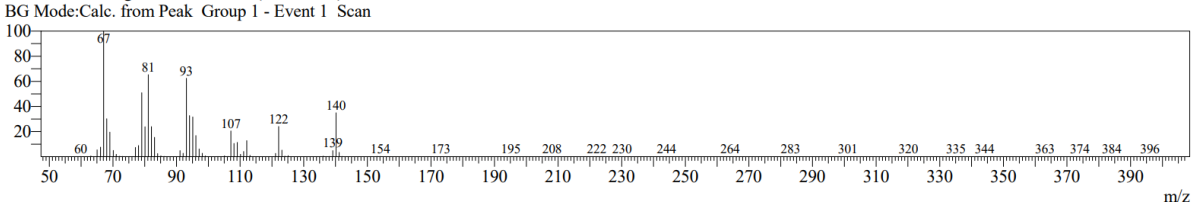

NMR spectra

6-Hydroxy-2H-pyran-3(6H)-one

^{1}H NMR (400 MHz, $CDCl_3$) δ 6.98 (dd, *J* = 10.4, 3.0 Hz, 1H), 6.18 (dd, *J* = 10.4, 1.0 Hz, 1H), 5.68 – 5.61 (m, 1H), 4.58 (d, *J* = 16.9 Hz, 1H), 4.15 (d, *J* = 16.9 Hz, 1H), 3.90 (d, *J* = 5.2 Hz, 1H).

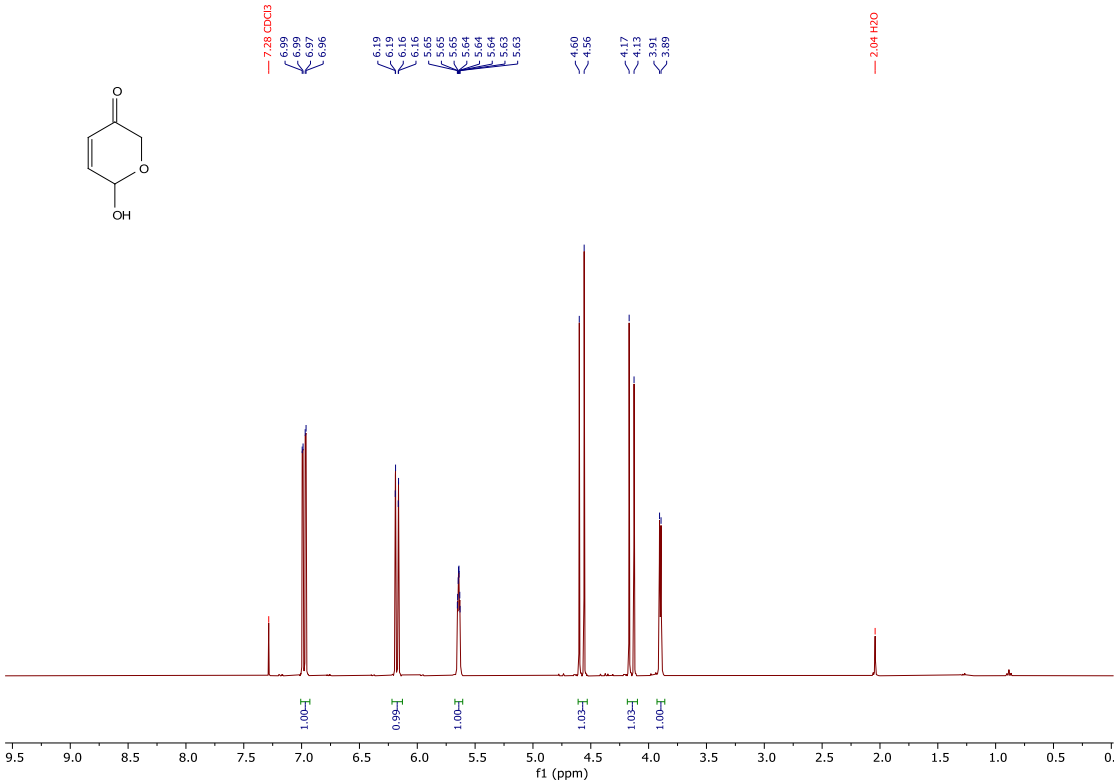

^{13}C NMR (101 MHz, $CDCl_3$) δ 194.91, 146.11, 127.84, 88.21, 66.61.

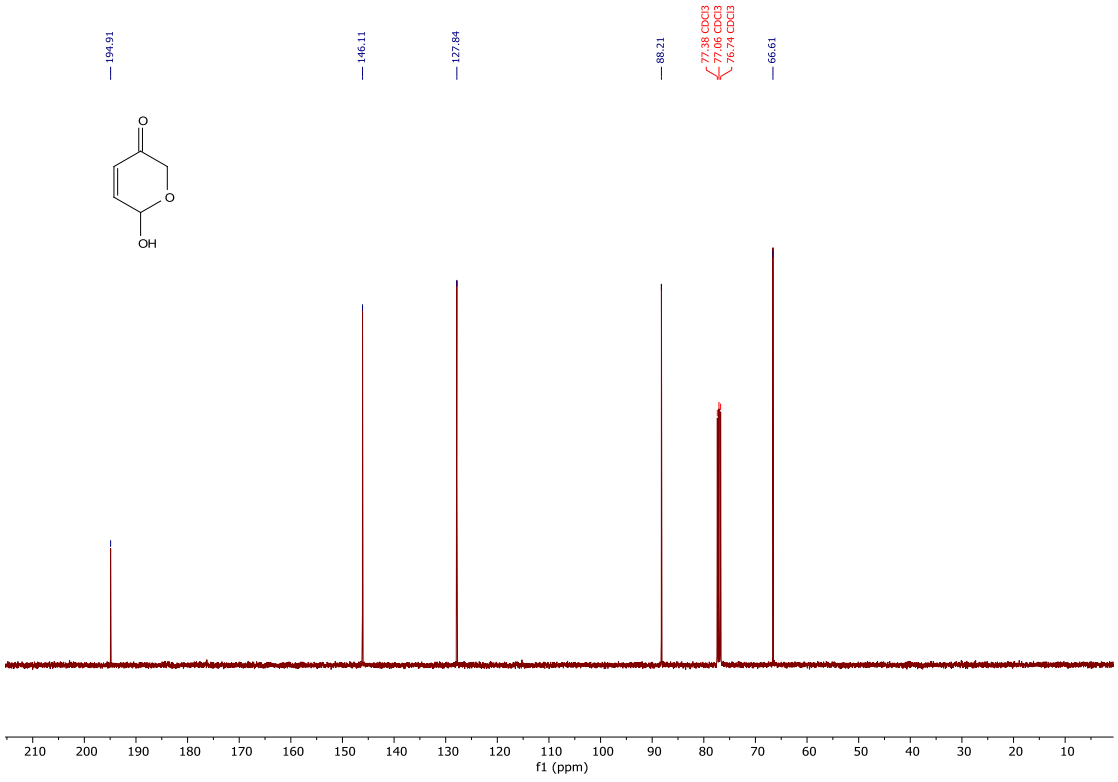

6-Methoxy-2H-pyran-3(6H)-one

^{1}H NMR (400 MHz, $CDCl_3$) δ 6.89 (dd, *J* = 10.3, 3.3 Hz, 1H), 6.14 (dd, *J* = 10.3, 0.8 Hz, 1H), 5.10 (d, *J* = 3.3 Hz, 1H), 4.45 (d, *J* = 16.8 Hz, 1H), 4.11 (d, *J* = 16.9 Hz, 1H), 3.53 (s, 3H).

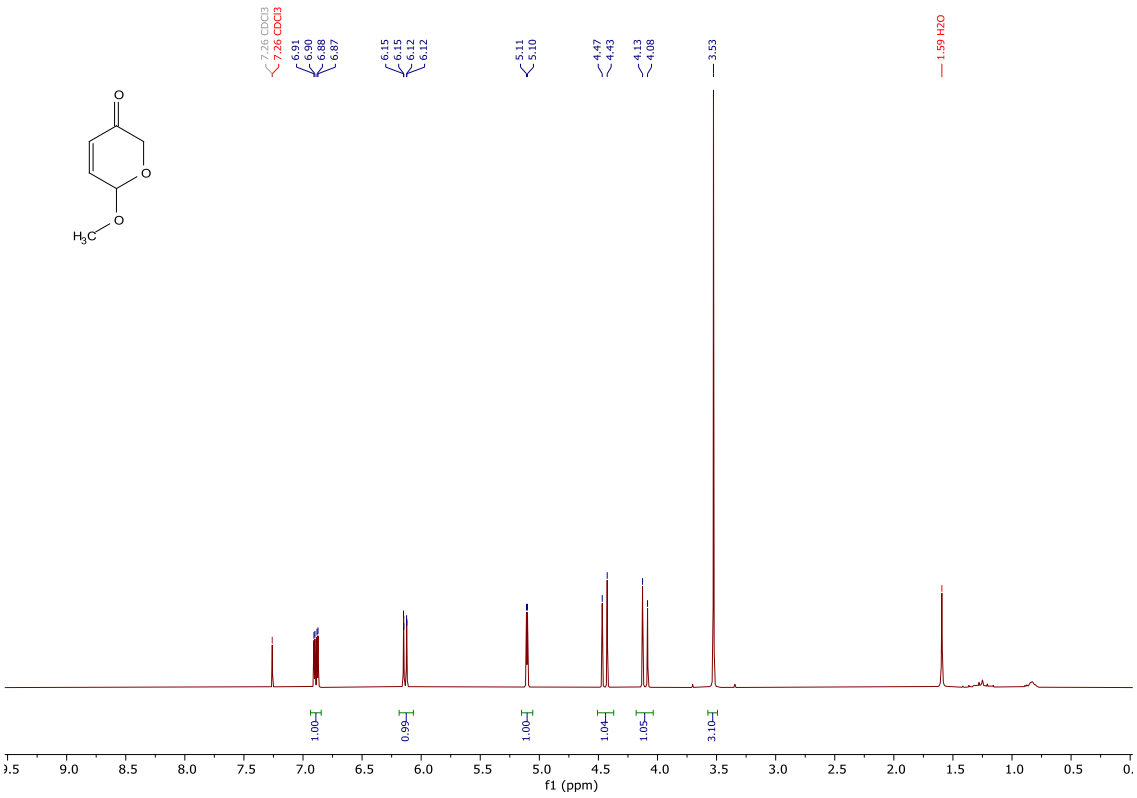

^{13}C NMR (101 MHz, $CDCl_3$) δ 194.72, 144.32, 127.96, 94.32, 66.33, 56.74.

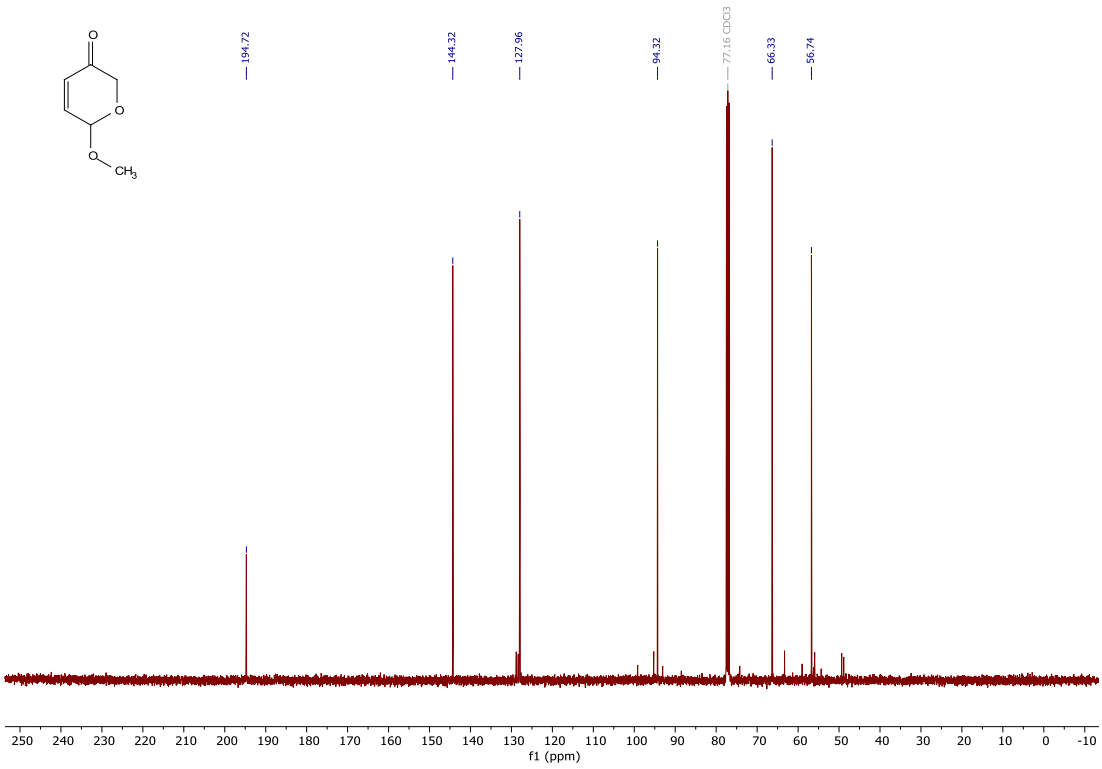

[2+2 cycloadducts]

HT cycloadduct (cycloadduct 3 in the main text)

^{1}H NMR (400 MHz, $CDCl_3$) δ 4.73 (d, *J* = 0.9 Hz, 2H), 4.18 (dd, *J* = 18.1, 0.7 Hz, 2H), 4.10 (d, *J* = 18.1 Hz, 2H), 3.40 (s, 6H), 3.23 – 3.16 (m, 2H), 2.91 – 2.82 (m, 2H).

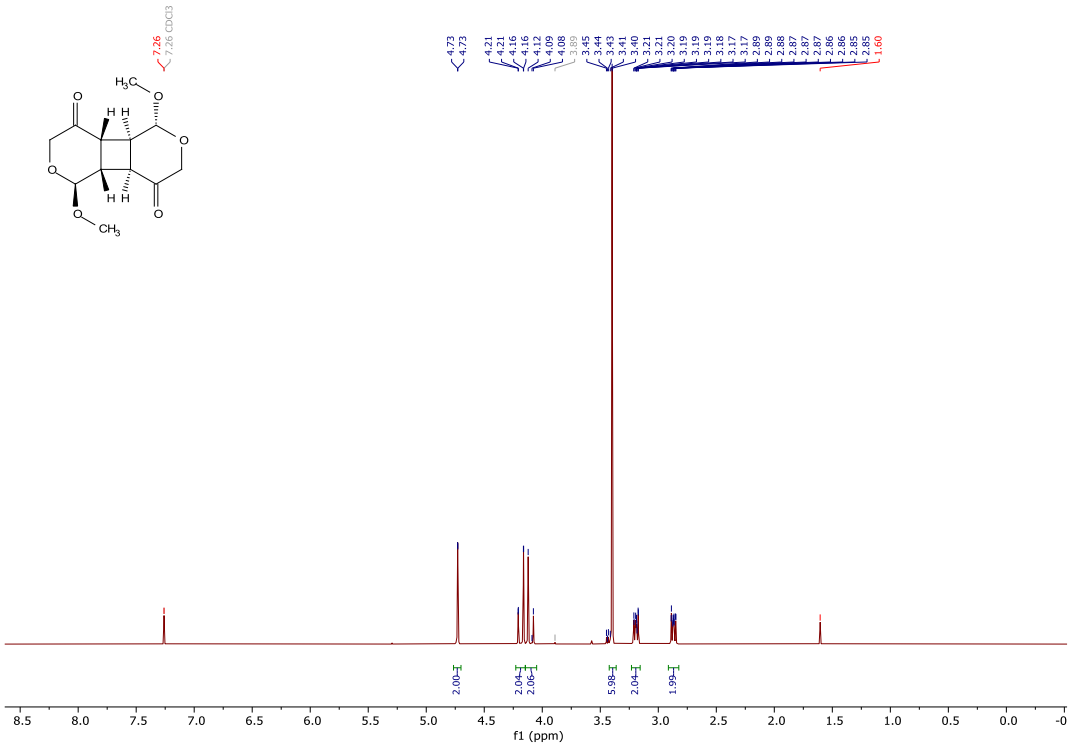

^{13}C NMR (101 MHz, $CDCl_3$) δ 207.56, 98.72, 65.57, 55.71, 41.63, 39.32.

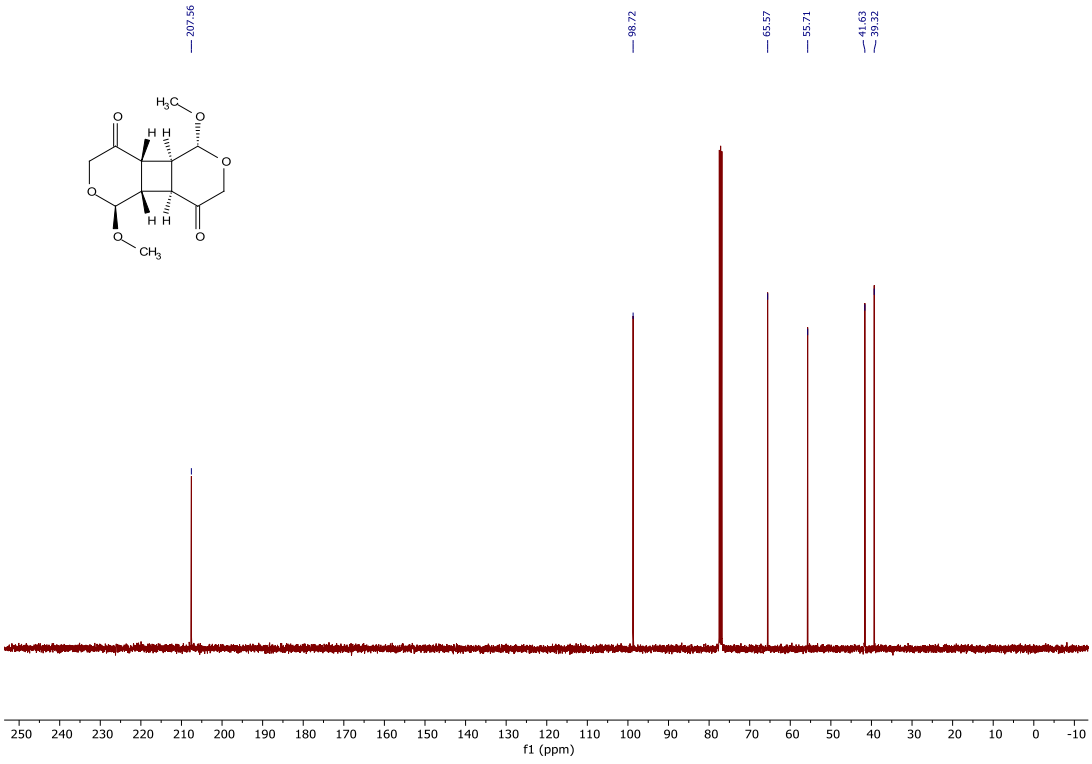

HH cycloadduct (cycloadduct 2 in the main text)

^{1}H NMR (400 MHz, $CDCl_3$) δ 4.72 (s, 2H), 4.24 (d, *J* = 17.9 Hz, 2H), 4.08 (d, *J* = 18.0 Hz, 2H), 3.41 (s, 6H), 3.24 – 3.16 (m, 2H), 2.87 – 2.78 (m, 2H).

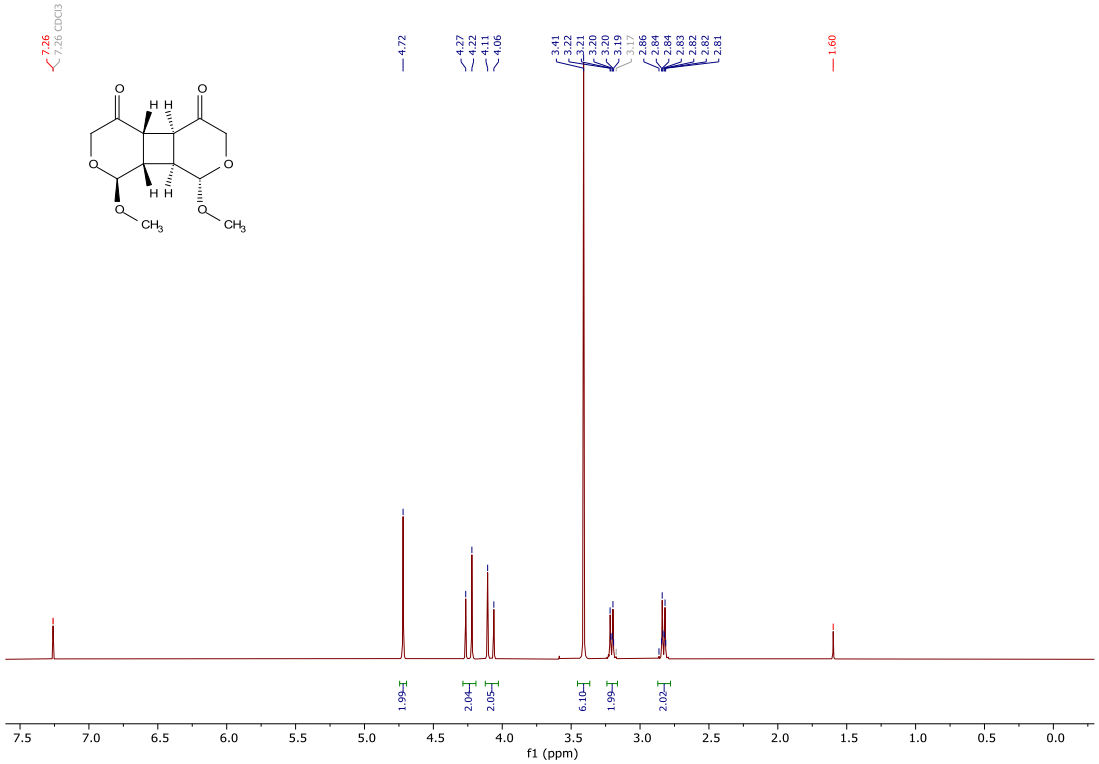

^{13}C NMR (101 MHz, $CDCl_3$) δ 205.63, 99.02, 65.51, 55.70, 41.24, 39.41.

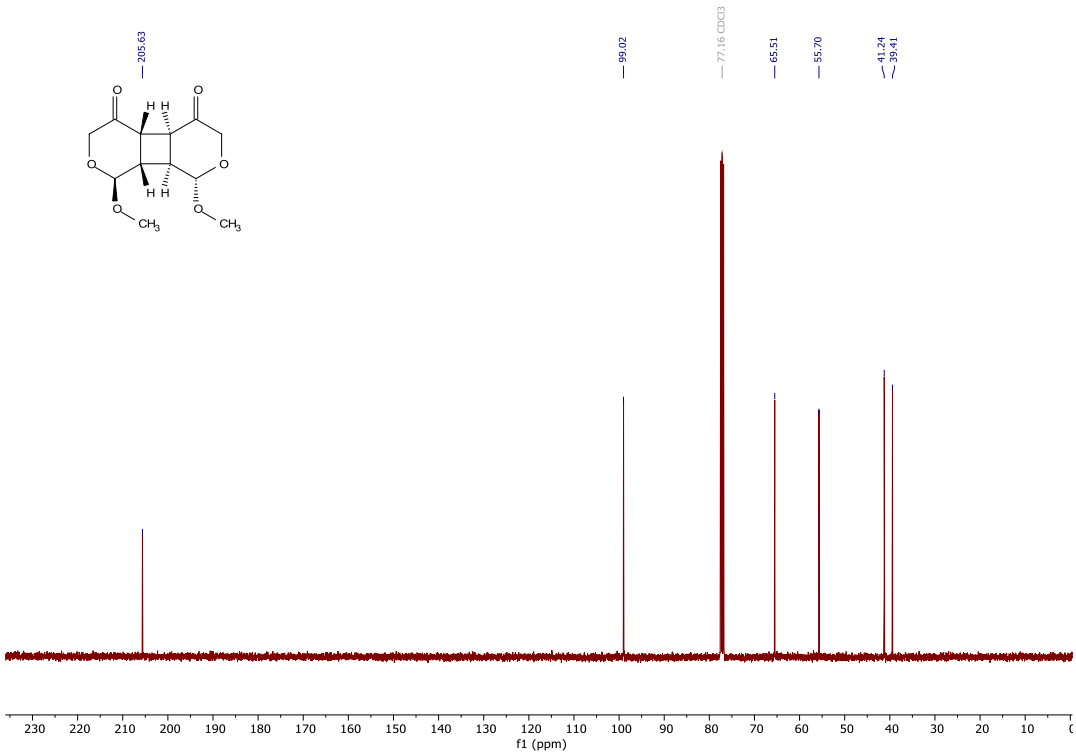

HH cycloadduct (cycloadduct 1 in the main text)

^{1}H NMR (400 MHz, $CDCl_3$) δ 4.74 (d, *J* = 3.9 Hz, 1H), 4.67 (d, *J* = 0.8 Hz, 1H), 4.28 (dd, *J* = 18.0, 0.9 Hz, 1H), 4.21 (dd, *J* = 17.9, 0.7 Hz, 1H), 4.06 (ddd, *J* = 18.0, 9.6, 0.7 Hz, 2H), 3.48 (s, 3H), 3.39 (s, 3H), 3.26 – 3.14 (m, 2H), 3.09 – 2.98 (m, 2H).

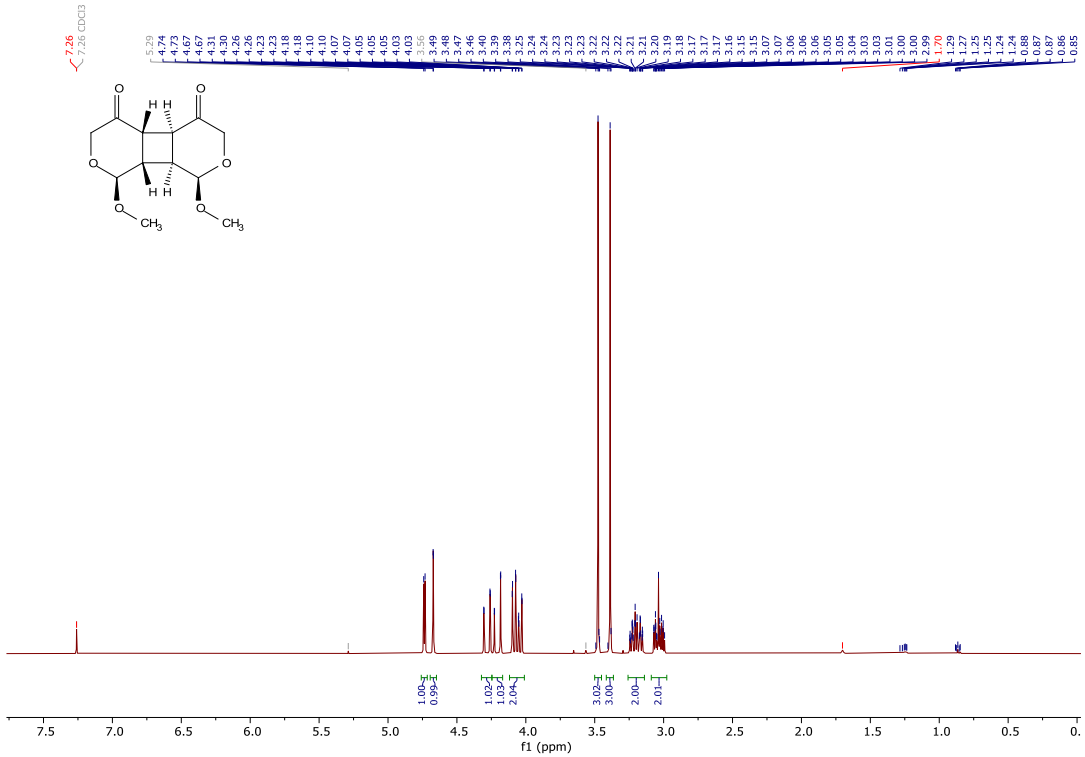

^{13}C NMR (101 MHz, $CDCl_3$) δ 206.86, 206.34, 99.37, 98.95, 69.68, 65.48, 56.46, 55.60, 43.00, 41.70, 38.97, 37.45.

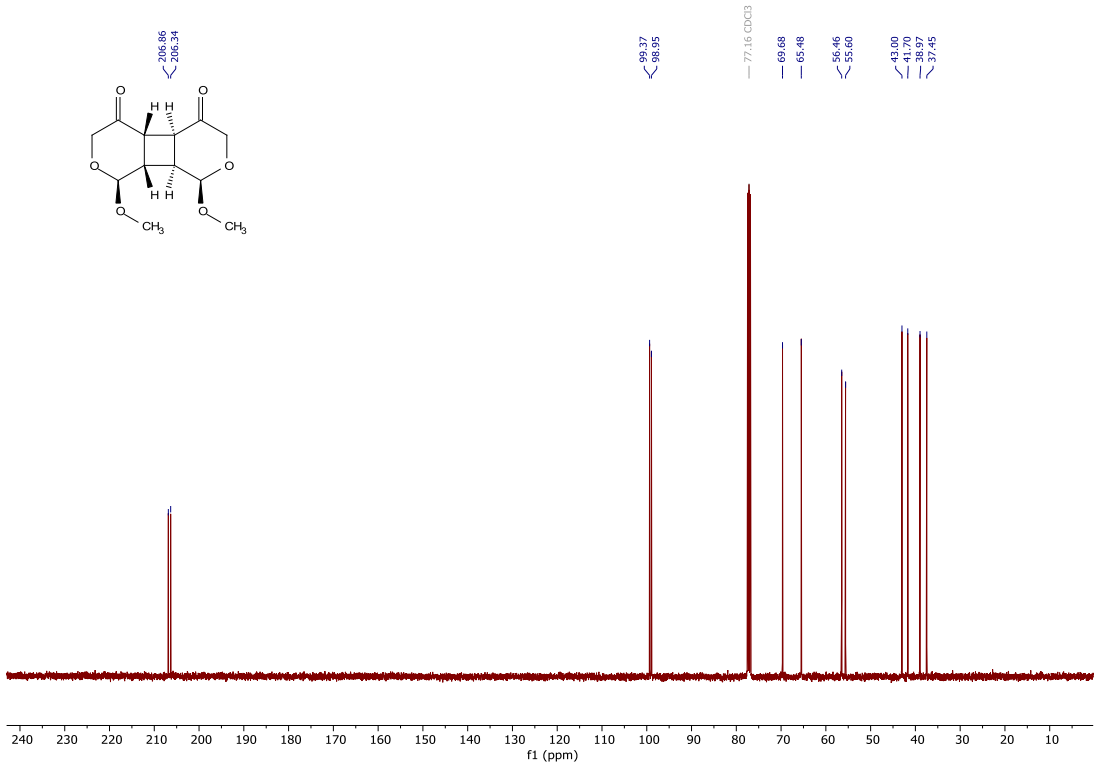

Life cycle assessment

The potential environmental impacts associated with the textile production from forestry biomass and the conversion of the hemicellulose in the pre-hydrolysis liquor to yield aviation fuels were evaluated through a Consequential Life Cycle Assessment (CLCA) following the four phases standard procedure by ISO 14040 and ISO 14044: Goal and scope definition, Inventory analysis, Impact assessment and Interpretation. The detailed methodology will follow in the next sections.

Goal and scope definition:

This LCA study aims to compare the environmental performances of a kraft mill producing regenerated cellulose for the dissolving grade pulp production used in the textile field, and an integrated kraft mill coupled with an upgrading process of hemicellulose to obtain cyclobutane-based aviation fuels.

In this conceptual design stage two scenarios are compared:

1. A first scenario (S1-Burn) representing the kraft pulping with a pre-hydrolysis stage for hemicellulose extraction and subsequent burning in a co-generation plant to generate heat and power from a bio-based material.
2. A second scenario (S2-AF) in which the hemicellulose extracted in the pre-hydrolysis section is upgraded to cyclobutane-based aviation fuels, the hemicellulose residues are burnt in a co-generation plant to deliver heat and power.

The aim is to investigate the environmental consequences associated with the extraction and upgrade of pre-hydrolysis liquor, a side-stream which is normally burnt with no added value.

According to the suggestions of ISO 14040 and ISO 14044, allocation has been avoided thanks to the consequential approach, allowing to account for all the chain effects when a change in the elementary flows or a change in the market occur.

The functional unit chosen was 1 kg of unbleached kraft pulp.

A cradle to gate approach was chosen excluding from our scope the bleaching step, the use phase, and the end life of the dissolving grade pulp. These phases of the life cycle are equal for both scenarios under study; thus, this approach will not affect the comparison according to ISO 14044.

The study is representative in a North Europe context (constituted by Sweden and Finland), with a broader European context investigated subsequently with in the sensitivity analysis.

To model the consumption and production electricity, an average of the marginal electricity of Sweden and Finland was considered, then for heat the substitution of biomass and coal were adopted for Sweden and Finland according to the procedure described by Marson et al.[3]

For kraft pulping processes, pre-hydrolysis liquor upgrading process to aviation fuels and product system a series of diagrams for system boundary are depicted in Figures S6 – S9.

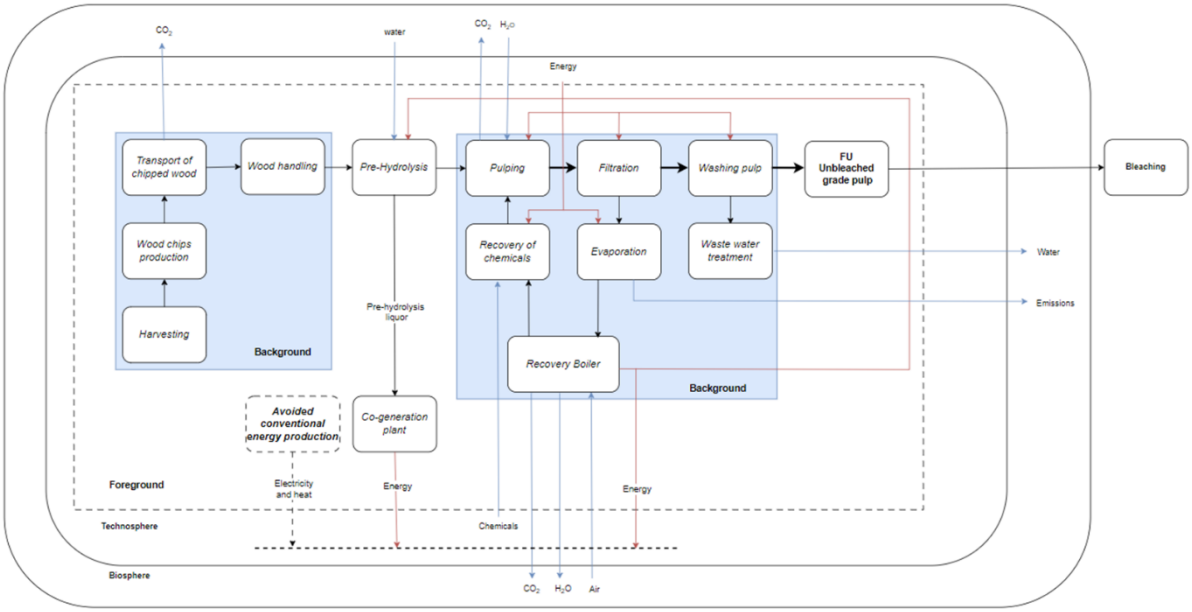

Figure S6. System boundaries for Scenario 1 (S1-Burn), hemicellulose extraction via pre-hydrolysis and incineration in co-generation plant for heat and power production.

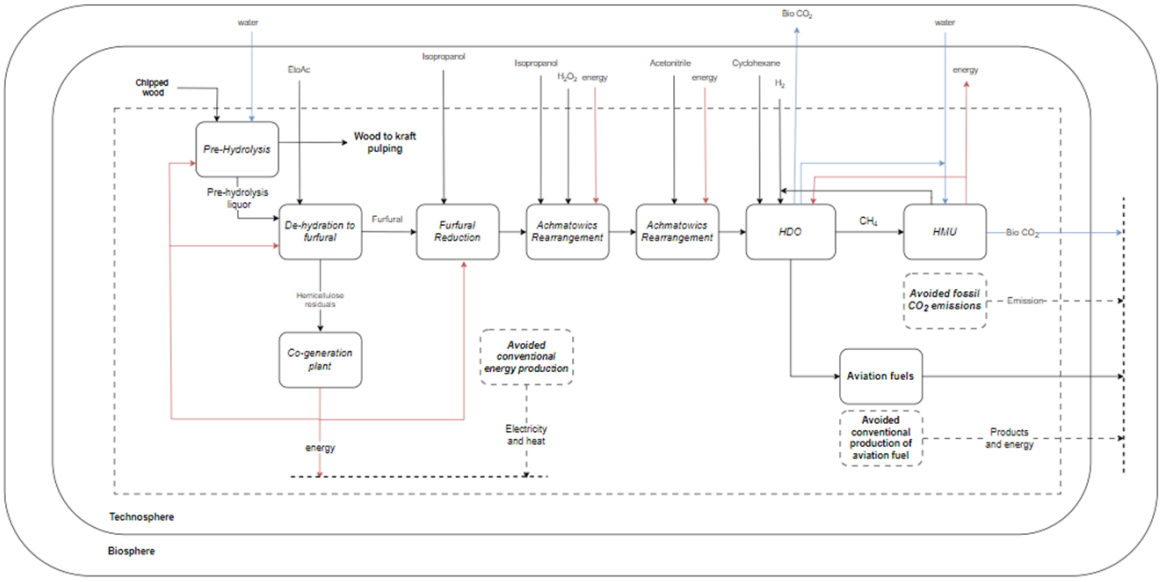

Figure S7. System boundaries for hemicellulose extraction via pre-hydrolysis and upgrade to biofuel for aviation, incineration of residues in co-generation plant for heat and power production.

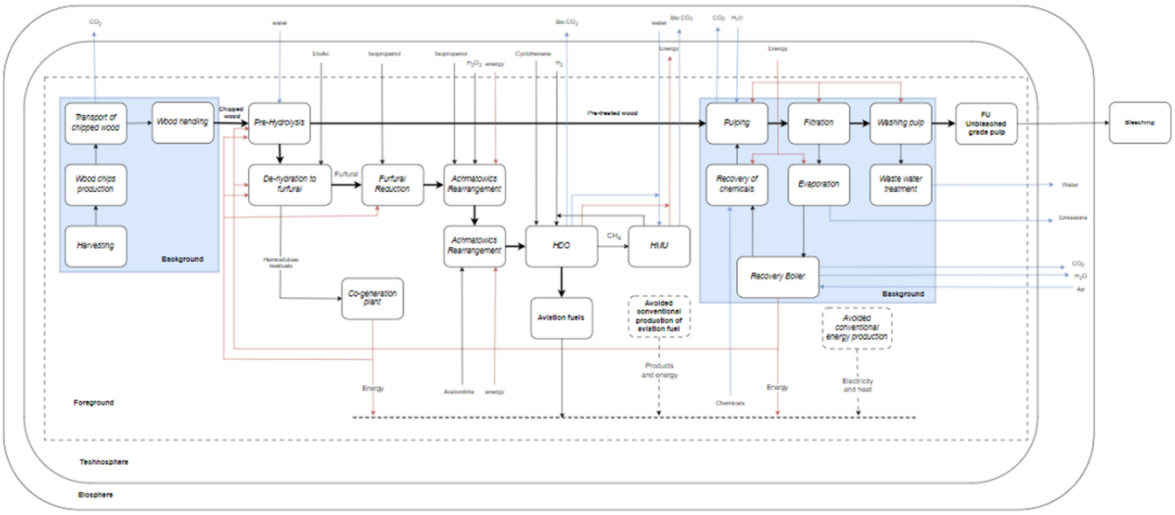

Figure S8. System boundaries for Scenario 2 (S2-AF), hemicellulose extraction, upgrade to aviation fuels and incineration in co-generation plant for heat and power production.

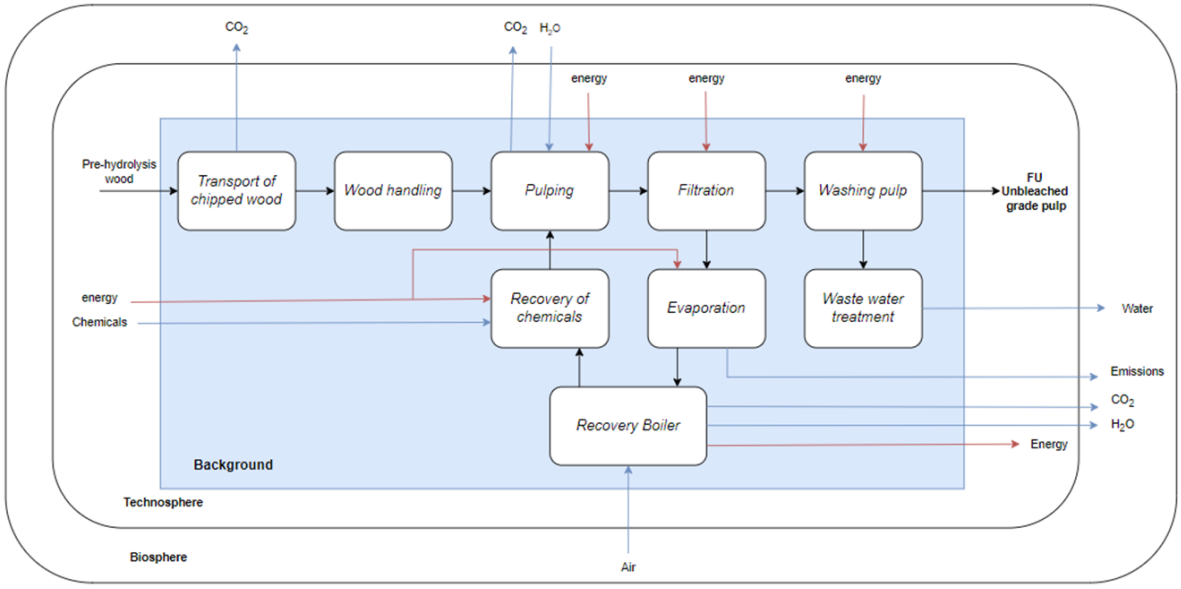

Figure S9. Kraft pulping process, treated with a black-box approach.

Data processing and system modelling was carried out using the LCA software SimaPro (v9.5.0.2) and background data from Ecoinvent 3.9.1 consequential. EF 3.0 version 1.01 (2019) was the methodology chosen for the impact assessment and the following impact categories were addressed in the study: climate change, land use, water use, resource use (fossil and minerals and metals). However, the other impact categories were also monitored: ozone depletion, ionizing radiation, photochemical ozone formation, particulate matter, human toxicity (cancer and non-cancer), acidification, eutrophication, ecotoxicity. The full set of impact categories and related units of measure is reported in Table S6.

Table S6. List of impact categories and related models

Impact category	Impact category indicator	Unit
Climate change	Radiative forcing as global warming potential	kg CO_2 eq
Ozone depletion	Ozone Depletion Potential	kg CFC 11 eq
Ionising radiation	Human exposure efficiency relative to U^{235}	kBq U-235 eq
Photochemical ozone formation	Tropospheric ozone concentration increase	kg NMVOC eq
Particulate matter	Impact on human health	disease inc.
Human toxicity, non-cancer	Comparative Toxic Unit for humans	CTUh
Human toxicity, cancer	Comparative Toxic Unit for humans	CTUh
Acidification	Accumulated Exceedance	mol H^+ eq
Eutrophication, freshwater	Fraction of nutrients reaching freshwater end compartment (P)	kg P eq
Eutrophication, marine	Fraction of nutrients reaching marine end compartment (N)	kg N eq
Eutrophication, terrestrial	Accumulated Exceedance	mol N eq
Ecotoxicity, freshwater	Comparative Toxic Unit for ecosystems	CTUe
Land use	This index is the result of the aggregation, performed by JRC, of the 4 indicators provided by LANCA model as indicators for land use (Soil quality index, Biotic production, Erosion resistance, Mechanical filtration, Groundwater replenishment)	Pt
Water use	User deprivation potential (deprivation-weighted water consumption)	m^3 depriv.
Resource use, fossils	Abiotic resource depletion – fossil fuels	MJ
Resource use, minerals and metals	Abiotic resource depletion	kg Sb eq

More information on the impact assessment models can be found in the following reference by Zampori *et al*.[4] It should be noted, however, that the LCA methodology is currently limited in the assessment of environmental aspects such as biodiversity, for which methodologies that can comprehensively capture all dimensions are not yet available.[5]

Inventory analysis

This LCA phase comprises the quantification and compilation of all the inputs and outputs related to the flows inside the product system through its entire Life Cycle or within the system boundaries.

A description of the sources of data used in the study can be found in Table S7. For the pulping process, secondary data was retrieved from ecoinvent 3.9.1 consequential and adapted to a hardwood-based starting material and neglecting all the chemicals involved in the bleaching step.

Table S7. Data sources.

	Data type	Data source
Kraft pulping dataset	Secondary	Ecoinvent 3.9.1 consequential
Birch wood composition	Primary	Laboratory
Yield to Unbleached pulp	Primary	Laboratory
Yield of pre-hydrolysis liquor	Primary	Laboratory
Yields in the aviation value chain	Primary	Laboratory
Yield to bio-based aviation fuels	Primary	Laboratory
Catalysts consumption	Calculated	Laboratory
Solvents and chemicals consumption	Calculated	Laboratory
Carbon content in wood fractions	Secondary	Ecoinvent 3.9.1 consequential
Low Heating Value of Black liquor	Secondary	Ecoinvent 3.9.1 consequential
Low Heating Value of hemicellulose	Secondary	(Furlan et al., 2013)
Low Heating of Value lignin	Secondary	(9)
Recovery boiler efficiency to heat and electricity.	Calculated	Ecoinvent 3.9.1 consequential
Co-generation plant efficiency to heat and electricity.	Secondary	Ecoinvent 3.9.1 conseqential

The calculation of scaling factors was the most conservative approach to adapt all the elementary flows to a hardwood biomass input, given that no datasets related to the production of unbleached pulp from hardwood were available. These scaling factors were calculated as the ratio between the total amount of wood input in the case of bleached pulp from hardwood and bleached pulp from softwood. The dataset was finally built applying a scaling factor of 0.89 for every elementary flow, except for “pulpwood, hardwood, measured as solid wood under bark” and “wood chips, wet, measured as dry mass” for which the scaling factors calculated were 1.03 and 0.234 respectively.

For all the unit processes involved in the hemicellulose upgrading primary data from laboratory previous analysis and measurements were used to build the mass and energy balances for inventory analysis.

Secondary data from Ecoinvent 3.9.1 consequential were exploited to determine the carbon content [kgC/kg] in cellulose, hemicellulose and lignin and their Low Heating Value [MJ/kg]. From the values retrieved the theoretical energy that can be produced was calculated and through secondary data from Ecoinvent 3.9.1 the efficiency of the recovery boiler was calculated to be 13% and used in the modelling of the scenarios.

For both S1-Burn and S2-AF secondary data for the values of efficiencies to heat and electricity from a co-generation plant were taken from Ecoinvent 3.9.1 and are 45% and 15% respectively.

The input and output data for the inventory analysis of this product system are listed in Table S8.

Table S8. Inventory input and output data for conversion of birch wood to unbleached pulp for dissolving grade pulp

FORESTRY HARVESTING			
Input	**value**	**Unit**	**Data source**
Birch wood	2,98	kg	Primary data
Diesel	0,00418	kg	Ecoinvent v3.9.1
Output			
Birch wood	2,98	kg	Primary data
CHIPPING			
Input	**Value**	**unit**	**Data source**
Birch wood	2,98	kg	Primary data
Diesel	0,005	kg	Ecoinvent v3.9.1
Output			
Birch wood chips	2,98	kg	Ecoinvent v3.9.1
PRE-HYDROLYSIS			
Input	**Value**	**unit**	**Data source**
Birch wood chips	2,98	kg	Primary data
Water, river	1,49	dm^3	Primary data
Output			
Wood without hemicellulose	2,26	kg	Primary data
Pre-hydrolysis liquor	0,723	kg	Primary data
Water, air emission	1,49	dm^3	Primary data
PULPING			
Input	**Value**	**Unit**	**Data source**
Wood without hemicellulose	2,26	kg	Primary data
Electricity	0,126	kWh	Secondary data
Other Chemicals			Secondary data
Output			
Unbleached pulp	1	kg	Primary data
Lignin	0.555	kg	Calculated data
Heat	1,119	MJ	Secondary data
Electricity	0,122	kWh	Secondary data
Emissions to air			Secondary data
Emissions to water			Secondary data
DE-HYDRATION			
Input	**Value**	**unit**	**Data source**

Pre-hydrolysis liquor	0,723	kg	Primary data
Ethyl acetate	0,0332	kg	Calculated data
Zeolites	0,000244	kg	Secondary data
Output			
Furfural	0,11	kg	Calculated data
Hemicellulose residuals	0,552	kg	Calculated data
Water	0,0619	dm^3	Calculated data
REDUCTION TO FURFURYL ALCOHOL			
Input	**value**	**unit**	**Data source**
Furfural	0.11	kg	Calculated data
Isopropanol	0.0715	kg	Calculated data
Hydrogen (make-up)	0,00224	kg	Calculated data
Au N-doped carbon	0.00250	kg	Calculated data
Output			
Furfuryl alcohol	0.111	kg	Calculated data
ACHMATOWICZ REARRANGEMENT			
Input	**value**	**unit**	**Data source**
Furfuryl alcohol	0.111	kg	Calculated data
Isopropanol	0.00185	kg	Calculated data
Hydrogen Peroxide (H_2O_2)	0.0384	kg	Calculated data
$MeReO_3$ catalyst	0.00284	kg	Calculated data
Zeolites as molecular sieves	0.111	kg	Calculated data
Output			
Rearrangement products	0.126	kg	Calculated data
Water	0.0204	kg	Calculated data
[2+2] CYCLOADDITION BY PHOTOCATALYSIS			
Input	**value**	**unit**	**Data source**
Rearrangement products	0.126	kg	Calculated data
Acetonitrile	0.0139	kg	Calculated data
Output			
Cycloadducts	0.121	kg	Calculated data
HYDROTREATMENT (HDO)			
Input	**value**	**unit**	**Data source**
Cycloadducts	0,121	kg	Calculated data
Cyclohexane	0.0127	kg	Calculated data
Hydrogen (make-up)	0,00335	kg	Calculated data
Ru catalyst	1,1E-07	kg	Ecoinvent v3.9.1
Zeolites	0,000244	kg	Ecoinvent v3.9.1
Output			

C10H20	0,00669	kg	Calculated data
C9H18	0,0121	kg	Calculated data
C8H16	0,00833	kg	Calculated data
C8-C10 ox.	2.13E-05	kmol	Calculated data
C7H14	0.00365	kg	Calculated data
Pentane	0,00115	kg	Calculated data
Methane	0.00571	kg	Calculated data

Primary data was used for the starting birch wood composition and the yields to Furfural.[6]
Primary data was used also for yields of cyclo-butane based aviation fuels from Furfural. The catalyst bed will be more consumed using the biofeed as compared to traditional fossil feeds such as vacuum gas oils: both because more material passes through the catalyst bed (factor 1.8) as well as the biofeed contains more oxygen and this will wear the catalyst by an estimated factor of 3 as compared to vacuum gas oils.[7] *Thus, all the input data of the database concerning the catalyst bed is multiplied by a factor of 5.4 to compensate for this.*

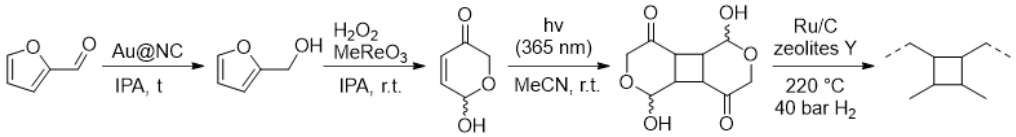

HYDROGEN MANUFACTURING UNIT (HMU)			
Input	**value**	**unit**	**Data source**
Methane	0,00571	kg	Calculated data
Water	0,0128	dm^3	Calculated data
Output			
CO_2 biogenic	0,0156	kg	Calculated data

The cyclobutane based products may undergo further hydrogenation to produce methane which can be reformed back to hydrogen gas and biogenic CO_2. This considerably lowers the demand of hydrogen introduced by the hydrogen make-up in the previous section:

$$CH_4 + 2H_2O \rightleftarrows CO_2 + 4H_2$$

INCINERATION in co-generation plant (S1-Burn)			
Input	**value**	**unit**	**Data source**
Lignin in black liquor	0,555	kg	Calculated data
Hemicellulose residuals	0,718	kg	Calculated data
Output			
Power	0,592	kWh	Calculated data
Heat	6.39	MJ	Calculated data

INCINERATION in co-generation plant (S2-AF)			
Input	**value**	**unit**	**Data source**
Lignin in black liquor	0,555	kg	Calculated data
Hemicellulose residuals	0,552	kg	Calculated data

Output			
Power	0,5	kWh	Calculated data
Heat	5,2	MJ	Calculated data

In S1-Burn and S2-AF the values of heat and power are a sum of the heat and power obtained from incineration of lignin in the Black liquor in the recovery boiler of the mill and the incineration of Pre-hydrolysis liquor (for S1-Burn) and hemicellulose residuals (S2-AF) in a co-generation plant with higher efficiency.

The values of the Lower Heating Value [MJ/kg] for lignin and hemicellulose comes from secondary data source.[8,9]

Impact assessment

Impact assessment was firstly performed to compare the impacts in the two scenarios, the results for all the impact categories and the variances between the cases are listed in Table S9. The 2nd Scenario (S2-AF) was the best performing in the climate change and mineral resources depletion impact categories, while the 1st Scenario (S1-Burn) was the most performing in the land use, water use and fossil resources depletion, highlighting that the implementation of a high-efficiency heat and power generation from biobased residues provide large benefits if compared to the counterpart exploiting the recovery boiler of the mill.

Table S9. Impact assessment of unbleached pulp production from S1-Burn and S2-AF.

Impact category	Unit	S1-Burn	S2-AF	Var% between S1 and S2
Climate change	kg CO_2 eq	2,34E-01	-5,63E-02	-515%
Ozone depletion	kg CFC 11 eq	4,29E-08	-2,27E-08	-289%
Ionising radiation	kBq U-235 eq	-2,00E-02	-2,29E-02	-13%
Photochemical ozone formation	kg NMVOC eq	2,18E-03	2,66E-03	18%
Particulate matter	disease inc.	3,22E-08	3,51E-08	8%
Human toxicity, non-cancer	CTUh	3,94E-09	1,56E-09	-153%
Human toxicity, cancer	CTUh	1,78E-10	6,18E-10	71%
Acidification	mol H^+ eq	2,10E-03	2,19E-03	4%
Eutrophication, freshwater	kg P eq	5,75E-05	1,64E-04	65%
Eutrophication, marine	kg N eq	7,57E-04	8,22E-04	8%
Eutrophication, terrestrial	mol N eq	9,04E-03	8,91E-03	-2%
Ecotoxicity, freshwater	CTUe	1,11E+01	5,18E+00	-114%
Land use	Pt	8,48E+01	1,72E+02	51%
Water use	m^3 depriv.	1,05E-01	3,69E-01	72%
Resource use, fossils	MJ	2,62E+00	5,16E+00	49%
Resource use, minerals and metals	kg Sb eq	4,06E-06	-6,44E-05	-106%

A contribution analysis was performed grouping together the main processes, in the specific the product system was divided in 7 groups:

- Raw materials: this group includes wood chips as a raw material for pulping, which is linked to the harvesting and chipping datasets, which are responsible for most of the impacts related to this group.
- Pulping and incineration: represents the dataset related to pulping, which include the chemicals involved in the kraft pulping process and all the emissions. In this group also the dataset related to the combustion of hemicellulose and the associated impacts are included.
- Solvents and chemicals: here are grouped together the solvents and chemicals needed in the aviation fuels production chain.
- Catalysis: address the impacts related to zeolites, molecular sieves and all the other catalysts involved in the aviation fuels production chain.
- Avoided products: comprises the products from the aviation fuels value chain, modelled as pentane and kerosene in SimaPro inventory.
- Avoided CO_2: comprises the datasets that model the avoided fossil CO_2 which is substituted with biogenic CO_2 when the aviation fuels are used and burned.
- Energy: comprises the consumption of energy and the avoid of energy from the grid, with the substitution with energy produced from biobased sources.

Such analysis was helpful since the benefits in climate change from production of energy from burning the residual biomass in a more efficient co-generation plant was large making difficult to understand the benefits from the avoided products and avoided fossil CO_2, a contribution analysis can disclose the results in a much clearer way. Tables S10 and S11 reports the outcomes of the contribution analysis regarding S1-Burn, while Tables S12-S13 show the contribution of every group to the overall impact in every impact category allowing a better understanding and interpretation of the results. In S1-Burn the key contributions to the environmental benefits in the different impact categories are given by the energy group, which is strongly dependent on the substituted mix and the geographical context. In S2-AF, the key contributions to the benefits arise mainly from the avoided aviation fuels from the conventional production and the avoided fossil CO_2 emissions at their end of life with the substitution of biogenic CO_2 emissions.

Table S10. Contribution analysis, kraft pulping with incineration in co-generation facility (S1-Burn Swedish + Finland scenario).

Impact category	Unit	Total	Raw materials	Pulping and incineration	Energy
Climate change	kg CO_2 eq	2,34E-01	6,60E-02	1,91E-01	-2,33E-02
Ozone depletion	kg CFC 11 eq	4,29E-08	1,40E-08	3,21E-08	-3,21E-09
Ionising radiation	kBq U-235 eq	-2,00E-02	3,76E-03	5,83E-03	-2,96E-02
Photochemical ozone formation	kg NMVOC eq	1,41E-03	5,27E-04	2,00E-03	-1,13E-03
Particulate matter	disease inc.	1,88E-08	2,36E-09	3,50E-08	-1,85E-08
Human toxicity, non-cancer	CTUh	3,77E-09	9,69E-10	8,86E-09	-6,06E-09
Human toxicity, cancer	CTUh	1,65E-10	5,90E-11	2,84E-10	-1,78E-10
Acidification	mol H^+ eq	1,45E-03	2,78E-04	2,61E-03	-1,44E-03
Eutrophication, freshwater	kg P eq	5,75E-05	1,27E-05	8,17E-05	-3,69E-05
Eutrophication, marine	kg N eq	4,58E-04	1,06E-04	7,45E-04	-3,93E-04
Eutrophication, terrestrial	mol N eq	5,76E-03	1,11E-03	1,11E-02	-6,40E-03
Ecotoxicity, freshwater	CTUe	1,04E+01	7,40E-01	2,41E+01	-1,44E+01
Land use	Pt	8,48E+01	1,53E+02	-1,78E+01	-5,09E+01
Water use	m^3 depriv.	1,05E-01	3,84E-03	1,16E-01	-1,45E-02
Resource use, fossils	MJ	2,62E+00	9,03E-01	1,96E+00	-2,44E-01
Resource use, minerals and metals	kg Sb eq	4,06E-06	-3,84E-07	6,43E-06	-1,99E-06

Table S11. Contribution analysis, kraft pulping with incineration in co-generation facility (S1-Burn European scenario).

Impact category	Unit	Total	Raw materials	Pulping and incineration	Energy
Climate change	kg CO_2 eq	1,91E-01	-8,92E-01	1,91E-01	-8,92E-01
Ozone depletion	kg CFC 11 eq	3,21E-08	2,08E-08	3,21E-08	2,08E-08
Ionising radiation	kBq U-235 eq	5,83E-03	-6,87E-03	5,83E-03	-6,87E-03
Photochemical ozone formation	kg NMVOC eq	2,00E-03	-2,74E-03	2,00E-03	-2,74E-03
Particulate matter	disease inc.	3,50E-08	-1,91E-08	3,50E-08	-1,91E-08
Human toxicity, non-cancer	CTUh	8,86E-09	-1,50E-08	8,86E-09	-1,50E-08
Human toxicity, cancer	CTUh	2,84E-10	-2,59E-10	2,84E-10	-2,59E-10
Acidification	mol H^+ eq	2,61E-03	-7,55E-03	2,61E-03	-7,55E-03
Eutrophication, freshwater	kg P eq	8,17E-05	-1,43E-03	8,17E-05	-1,43E-03
Eutrophication, marine	kg N eq	7,45E-04	-1,20E-03	7,45E-04	-1,20E-03
Eutrophication, terrestrial	mol N eq	1,11E-02	-1,15E-02	1,11E-02	-1,15E-02
Ecotoxicity, freshwater	CTUe	2,41E+01	-1,92E+01	2,41E+01	-1,92E+01
Land use	Pt	-1,78E+01	-3,25E+01	-1,78E+01	-3,25E+01
Water use	m^3 depriv.	1,16E-01	-1,45E-01	1,16E-01	-1,45E-01
Resource use, fossils	MJ	1,96E+00	-8,70E+00	1,96E+00	-8,70E+00
Resource use, minerals and metals	kg Sb eq	6,43E-06	3,25E-06	6,43E-06	3,25E-06

Table S12. Contribution analysis, cyclobutane based biofuels production (S2-AF Swedish + Finland scenario).

Impact category	Unit	Total	Raw materials	Pulping and incineration	Catalysts	Chemicals and solvents	Avoided products	Energy	Avoided CO2
Climate change	kg CO_2 eq	-5,65E-02	8,72E-02	2,75E-01	6,38E-03	2,35E-01	-9,01E-02	4,86E-04	-5,70E-01
Ozone depletion	kg CFC 11 eq	-2,27E-08	1,85E-08	5,39E-08	1,54E-09	5,08E-08	-1,47E-07	-3,77E-10	0,00E+00
Ionising radiation	kBq U-235 eq	-2,29E-02	4,97E-03	-3,98E-03	5,04E-03	9,13E-03	-3,80E-02	-3,12E-05	0,00E+00
Photochemical ozone formation	kg NMVOC eq	1,88E-03	6,96E-04	1,36E-03	-9,92E-05	7,54E-04	-6,04E-04	-2,20E-04	0,00E+00
Particulate matter	disease inc.	2,17E-08	3,12E-09	1,89E-08	1,30E-10	8,51E-09	-5,34E-09	-3,64E-09	0,00E+00
Human toxicity, non-cancer	CTUh	1,40E-09	1,28E-09	4,05E-09	-3,27E-09	1,42E-09	-1,10E-09	-9,82E-10	0,00E+00
Human toxicity, cancer	CTUh	6,05E-10	7,79E-11	1,63E-10	2,88E-10	1,40E-10	-3,84E-11	-2,57E-11	0,00E+00
Acidification	mol H^+ eq	1,55E-03	3,68E-04	1,59E-03	-3,32E-04	1,12E-03	-9,16E-04	-2,79E-04	0,00E+00
Eutrophication, freshwater	kg P eq	1,64E-04	1,68E-05	6,18E-05	6,23E-05	3,93E-05	-1,12E-05	-5,34E-06	0,00E+00
Eutrophication, marine	kg N eq	5,23E-04	1,40E-04	4,49E-04	-1,71E-05	1,59E-04	-1,31E-04	-7,77E-05	0,00E+00
Eutrophication, terrestrial	mol N eq	5,63E-03	1,46E-03	5,59E-03	-3,76E-04	1,68E-03	-1,44E-03	-1,30E-03	0,00E+00
Ecotoxicity, freshwater	CTUe	4,50E+00	9,77E-01	1,17E+01	-2,76E+00	2,37E+00	-4,96E+00	-2,78E+00	0,00E+00
Land use	Pt	1,72E+02	2,03E+02	-1,83E+01	-6,46E-01	3,96E-01	-1,16E+00	-1,07E+01	0,00E+00
Water use	m^3 depriv.	3,69E-01	5,07E-03	1,40E-01	1,11E-01	1,17E-01	-3,71E-03	-2,50E-04	0,00E+00
Resource use, fossils	MJ	5,16E+00	1,19E+00	4,94E+00	1,82E-01	8,08E+00	-9,36E+00	1,21E-01	0,00E+00
Resource use, minerals and metals	kg Sb eq	-6,44E-05	-5,07E-07	5,29E-06	-7,18E-05	1,99E-06	6,67E-09	6,11E-07	0,00E+00

Table S13. Contribution analysis, cyclobutane based biofuels production (S2-AF European scenario).

Impact category	Unit	Total	Raw materials	Pulping and incineration	Catalysts	Chemicals and solvents	Avoided products	Energy	Avoided CO2
Climate change	kg CO_2 eq	-2,32E-01	8,72E-02	2,75E-01	6,38E-03	2,35E-01	-9,01E-02	-1,75E-01	-5,70E-01
Ozone depletion	kg CFC 11 eq	-1,61E-08	1,85E-08	5,39E-08	1,54E-09	5,08E-08	-1,47E-07	6,24E-09	0,00E+00
Ionising radiation	kBq U-235 eq	-1,66E-02	4,97E-03	-3,98E-03	5,04E-03	9,13E-03	-3,80E-02	6,30E-03	0,00E+00
Photochemical ozone formation	kg NMVOC eq	1,55E-03	6,96E-04	1,36E-03	-9,92E-05	7,54E-04	-6,04E-04	-5,49E-04	0,00E+00
Particulate matter	disease inc.	2,16E-08	3,12E-09	1,89E-08	1,30E-10	8,51E-09	-5,34E-09	-3,69E-09	0,00E+00
Human toxicity, non-cancer	CTUh	-6,49E-10	1,28E-09	4,05E-09	-3,27E-09	1,42E-09	-1,10E-09	-3,03E-09	0,00E+00
Human toxicity, cancer	CTUh	5,84E-10	7,79E-11	1,63E-10	2,88E-10	1,40E-10	-3,84E-11	-4,75E-11	0,00E+00
Acidification	mol H^+ eq	2,95E-04	3,68E-04	1,59E-03	-3,32E-04	1,12E-03	-9,16E-04	-1,53E-03	0,00E+00
Eutrophication, freshwater	kg P eq	-1,28E-04	1,68E-05	6,18E-05	6,23E-05	3,93E-05	-1,12E-05	-2,96E-04	0,00E+00
Eutrophication, marine	kg N eq	3,57E-04	1,40E-04	4,49E-04	-1,71E-05	1,59E-04	-1,31E-04	-2,43E-04	0,00E+00
Eutrophication, terrestrial	mol N eq	4,60E-03	1,46E-03	5,59E-03	-3,76E-04	1,68E-03	-1,44E-03	-2,33E-03	0,00E+00
Ecotoxicity, freshwater	CTUe	3,37E+00	9,77E-01	1,17E+01	-2,76E+00	2,37E+00	-4,96E+00	-3,91E+00	0,00E+00
Land use	Pt	1,76E+02	2,03E+02	-1,83E+01	-6,46E-01	3,96E-01	-1,16E+00	-6,57E+00	0,00E+00
Water use	m^3 depriv.	3,42E-01	5,07E-03	1,40E-01	1,11E-01	1,17E-01	-3,71E-03	-2,76E-02	0,00E+00
Resource use, fossils	MJ	3,54E+00	1,19E+00	4,94E+00	1,82E-01	8,08E+00	-9,36E+00	-1,50E+00	0,00E+00
Resource use, minerals and metals	kg Sb eq	-6,40E-05	-5,07E-07	5,29E-06	-7,18E-05	1,99E-06	6,67E-09	1,05E-06	0,00E+00

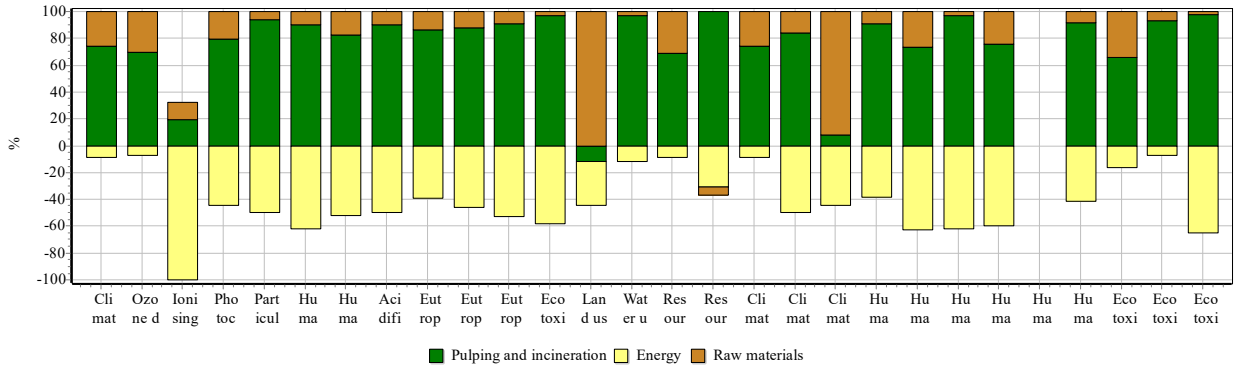

Figure S10: Contribution analysis outcome, S1-Burn, Swedish and Finland mix.

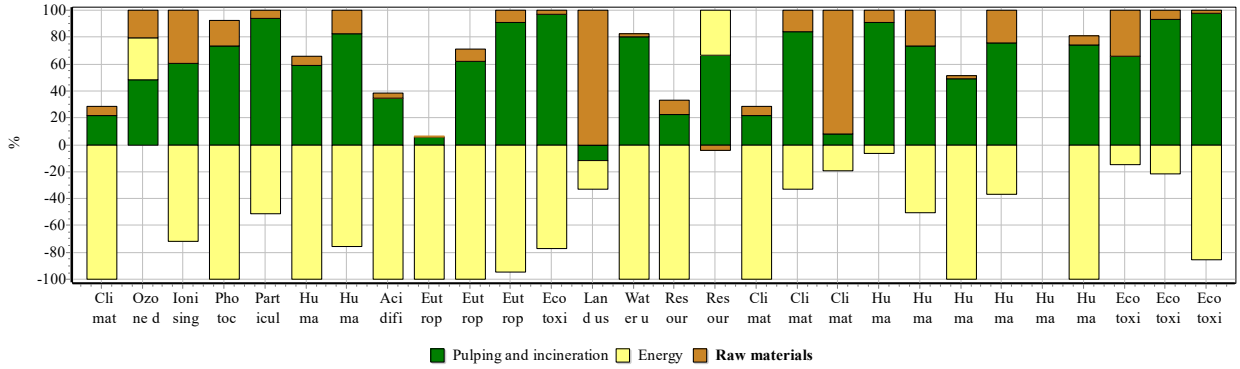

Figure S11: Contribution analysis outcome, S1-Burn, average European mix.

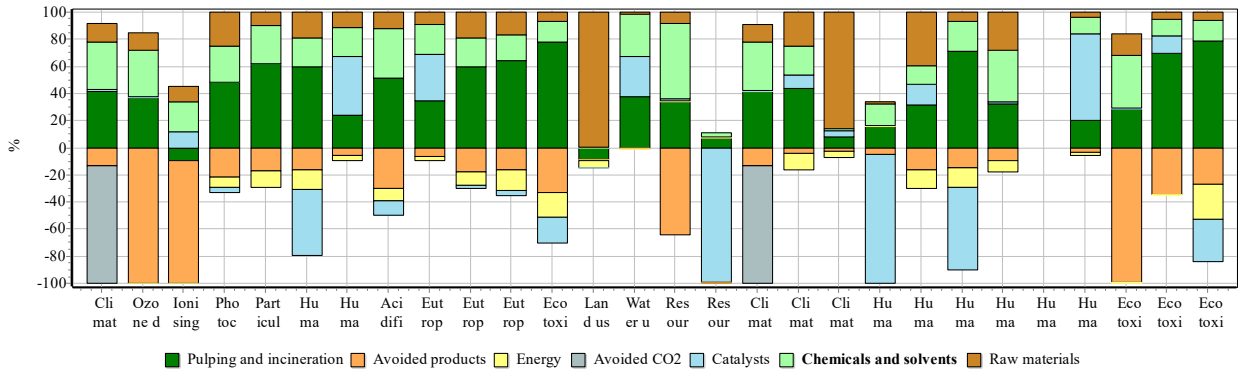

Figure S12: Contribution analysis outcome, S2-AF, Swedish and Finland mix.

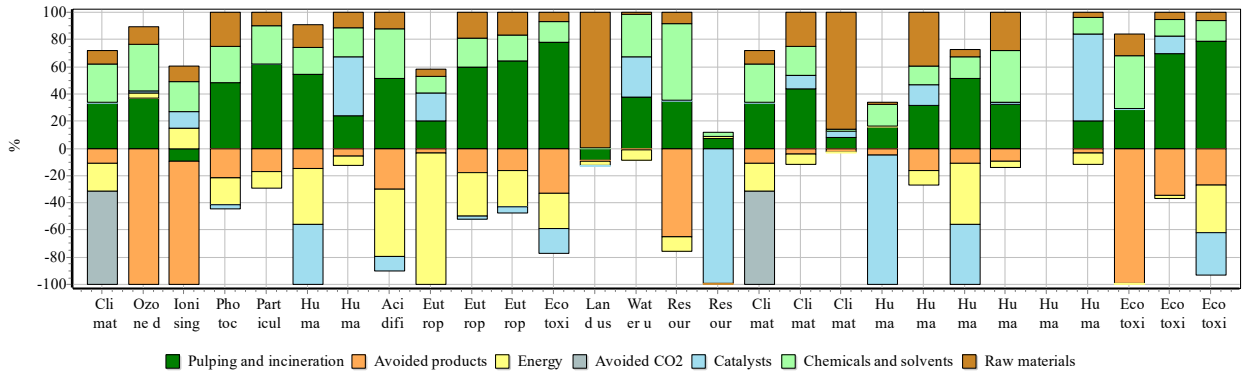

Figure S13: Contribution analysis outcome, S2-AF, average European mix.

Sensitivity analysis

The aim of the sensitivity analysis is to investigate the influence of different modelling and operating choices on the Scenarios, i.e. the sensitivity of the Scenarios when some parameters representing the modelling strategies are manipulated.

A first sensitivity analysis on the product system proposed was performed by a change in the location of the integrated pulp mill to an average European scenario, switching to a European network for heat and electricity.

Significant variations were obtained for both scenarios, with large environmental benefits in the climate change, water use and fossil resource use categories. The effect on climate change can be attributed to the higher emission factor of the average European energy mix (0.218 $kgCO_2eq/kWh$ of electricity versus 0.07 $kgCO_2eq/kWh$ for the Northern mix), resulting in large benefits. This leads to an overall reduction of GHG emissions for both scenarios when an energy mix with high shares of fossil resources is substituted. The results reported in Table S14 shows that locating the integrated pulp mill in an average European context improve the environmental performances in the climate change, water use and resource use impact categories, but it is slightly worse for the land use impact category.

Table S14. Sensitivity analysis comparing Swedish + Finnish scenario to a European scenario.

S1-Burn				
Impact category	**Unit**	**Swedish + Finnish scenario**	**European scenario**	**Var%**
Climate change	kg CO_2 eq	2,34E-01	-6,34E-01	-371%
Ozone depletion	kg CFC 11 eq	4,29E-08	6,69E-08	56%
Ionising radiation	kBq U-235 eq	-2,00E-02	2,73E-03	114%
Photochemical ozone formation	kg NMVOC eq	2,18E-03	5,62E-04	-74%
Particulate matter	disease inc.	3,22E-08	3,16E-08	-2%
Human toxicity, non-cancer	CTUh	3,94E-09	-4,96E-09	-226%
Human toxicity, cancer	CTUh	1,78E-10	9,65E-11	-46%
Acidification	mol H^+ eq	2,10E-03	-4,01E-03	-291%
Eutrophication, freshwater	kg P eq	5,75E-05	-1,34E-03	-2426%
Eutrophication, marine	kg N eq	7,57E-04	-4,96E-05	-107%
Eutrophication, terrestrial	mol N eq	9,04E-03	3,91E-03	-57%
Ecotoxicity, freshwater	CTUe	1,11E+01	6,28E+00	-43%
Land use	Pt	8,48E+01	1,03E+02	22%
Water use	m^3 depriv.	1,05E-01	-2,54E-02	-124%
Resource use, fossils	MJ	2,62E+00	-5,83E+00	-323%
Resource use, minerals and metals	kg Sb eq	4,06E-06	9,30E-06	129%
S2-AF				
Impact category	**Unit**	**Swedish + Finnish scenario**	**European scenario**	**Var%**
Climate change	kg CO_2 eq	-5,63E-02	-2,32E-01	-311%
Ozone depletion	kg CFC 11 eq	-2,27E-08	-1,61E-08	29%
Ionising radiation	kBq U-235 eq	-2,29E-02	-1,66E-02	28%
Photochemical ozone formation	kg NMVOC eq	2,66E-03	2,33E-03	12%
Particulate matter	disease inc.	3,51E-08	3,51E-08	0%
Human toxicity, non-cancer	CTUh	1,56E-09	-4,84E-10	131%
Human toxicity, cancer	CTUh	6,18E-10	5,96E-10	4%

Acidification	mol H^+ eq	2,19E-03	9,40E-04	57%
Eutrophication, freshwater	kg P eq	1,64E-04	-1,28E-04	178%
Eutrophication, marine	kg N eq	8,22E-04	6,56E-04	20%
Eutrophication, terrestrial	mol N eq	8,91E-03	7,87E-03	12%
Ecotoxicity, freshwater	CTUe	5,18E+00	4,05E+00	22%
Land use	Pt	1,72E+02	1,76E+02	2%
Water use	m^3 depriv.	3,69E-01	3,42E-01	-7%
Resource use, fossils	MJ	5,16E+00	3,54E+00	-31%
Resource use, minerals and metals	kg Sb eq	-6,44E-05	-6,40E-05	1%

Sensitivity analysis was implemented also to investigate a worse scenario where the yields to aviation fuels (modelled as kerosene) are decreased by 10%, assuming a constant yield of unbleached grade pulp. The results in Table S15 shows that the GWP-total and the ADP-fossil indicators got worse, but from a climate change point of view, S2-AF still delivers a better performance than S1-Burn, while it still have higher impacts regarding the use of fossil resources.

Table S15. Sensitivity analysis when the cyclobutane based biofuels: yield decreased by 10%.

		S2-AF		
Impact category	**Unit**	**Proposed Scenario**	**Lower yield scenario**	**Var%**
Climate change	kg CO_2 eq	-5,63E-02	6,59E-03	112%
Ozone depletion	kg CFC 11 eq	-2,27E-08	-1,25E-08	45%
Ionising radiation	kBq U-235 eq	-2,29E-02	-2,02E-02	12%
Photochemical ozone formation	kg NMVOC eq	2,66E-03	2,70E-03	2%
Particulate matter	disease inc.	3,51E-08	3,54E-08	1%
Human toxicity, non-cancer	CTUh	1,56E-09	1,64E-09	5%
Human toxicity, cancer	CTUh	6,18E-10	6,20E-10	0%
Acidification	mol H^+ eq	2,19E-03	2,25E-03	3%
Eutrophication, freshwater	kg P eq	1,64E-04	1,64E-04	0%
Eutrophication, marine	kg N eq	8,22E-04	8,31E-04	1%
Eutrophication, terrestrial	mol N eq	8,91E-03	9,01E-03	1%

Ecotoxicity, freshwater	CTUe	5,18E+00	5,54E+00	7%
Land use	Pt	1,72E+02	1,72E+02	0%
Water use	m^3 depriv.	3,69E-01	3,70E-01	0%
Resource use, fossils	MJ	5,16E+00	5,83E+00	13%
Resource use, minerals and metals	kg Sb eq	-6,44E-05	-6,44E-05	0%

Another sensitivity analysis was useful to understand the consequences in decoupling the upgrading process from the kraft pulp mill, in this scenario another facility would buy the pre-hydrolysis liquor from the kraft pulp mill and couldn't exploit the energy retrieved from the mill to run the unit processes in the upgrading value chain. From Table S16 a small benefit can be disclosed in the climate change and benefits in the resource use impact category are shown when decoupling the cyclobutane-based fuels to the kraft mill. The small difference may be explained with a balance in the energy from the grid, the energy from the grid that is used in the upgrading process is balanced by the energy produced and exported by the kraft mill, thus the overall impacts are counterbalanced.

Table S16. Sensitivity analysis when upgrading hemicellulose in a separate plant.

S2-AF				
Impact category	**Unit**	**Integrated pulp mill scenario**	**Independent plant scenario**	**Var%**
Climate change	kg CO_2 eq	-5,63E-02	-5,81E-02	-3%
Ozone depletion	kg CFC 11 eq	-2,27E-08	-1,94E-08	15%
Ionising radiation	kBq U-235 eq	-2,29E-02	-2,00E-02	13%
Photochemical ozone formation	kg NMVOC eq	2,66E-03	4,52E-03	70%
Particulate matter	disease inc.	3,51E-08	6,58E-08	87%
Human toxicity, non-cancer	CTUh	1,56E-09	9,95E-09	538%
Human toxicity, cancer	CTUh	6,18E-10	8,39E-10	36%
Acidification	mol H^+ eq	2,19E-03	4,55E-03	108%
Eutrophication, freshwater	kg P eq	1,64E-04	2,10E-04	28%
Eutrophication, marine	kg N eq	8,22E-04	1,48E-03	80%
Eutrophication, terrestrial	mol N eq	8,91E-03	1,98E-02	123%
Ecotoxicity, freshwater	CTUe	5,18E+00	2,87E+01	454%
Land use	Pt	1,72E+02	2,62E+02	52%
Water use	m^3 depriv.	3,69E-01	3,73E-01	1%
Resource use, fossils	MJ	5,16E+00	4,22E+00	-18%
Resource use, minerals and metals	kg Sb eq	-6,44E-05	-6,91E-05	7%

A last sensitivity analysis was carried out to see the influence on the results when changing the impact assessment method from the EF Method 3.0 to ReCiPe, 2016, (midpoint) H. In this method the following impact categories were addressed: global warming, water consumption, land use, mineral resource scarcity and fossil resource scarcity, but all the impact categories are as well reported in Table S17. For the interested impact categories for this study a small difference, not significant, can be disclosed when switching to the ReCiPe, 2016 (midpoint), H method.

Table S17. Sensitivity analysis comparing the different scenarios using ReCiPe 2016 (Midpoint), H.

Impact category	**Unit**	**S1-Burn**	**S2-AF**	**Var% between S1-Burn and S2-AF**
Global warming	kg CO2 eq	2,33E-01	-5,94E-02	-126%
Stratospheric ozone depletion	kg CFC11 eq	8,92E-08	-2,41E-09	-103%
Ionizing radiation	kBq Co-60 eq	-2,62E-02	-1,18E-02	55%
Ozone formation, Human health	kg NOx eq	1,95E-03	2,12E-03	9%
Fine particulate matter formation	kg PM2.5 eq	5,38E-04	5,74E-04	7%
Ozone formation, Terrestrial ecosystems	kg NOx eq	1,98E-03	2,18E-03	10%
Terrestrial acidification	kg SO2 eq	1,19E-03	1,25E-03	5%
Freshwater eutrophication	kg P eq	5,01E-04	5,78E-04	15%
Marine eutrophication	kg N eq	1,96E-06	1,02E-05	419%
Terrestrial ecotoxicity	kg 1,4-DCB	1,16E+00	-3,74E-02	-103%
Freshwater ecotoxicity	kg 1,4-DCB	1,79E-04	6,00E-02	33351%
Marine ecotoxicity	kg 1,4-DCB	1,62E-03	7,49E-02	4508%
Human carcinogenic toxicity	kg 1,4-DCB	1,05E-02	1,75E-02	66%
Human non-carcinogenic toxicity	kg 1,4-DCB	2,04E-01	6,70E-01	229%
Land use	m2a crop eq	7,58E-01	1,53E+00	101%
Mineral resource scarcity	kg Cu eq	6,15E-04	1,14E-02	1746%
Fossil resource scarcity	kg oil eq	7,48E-02	1,28E-01	72%
Water consumption	m3	8,10E-04	9,42E-03	1064%

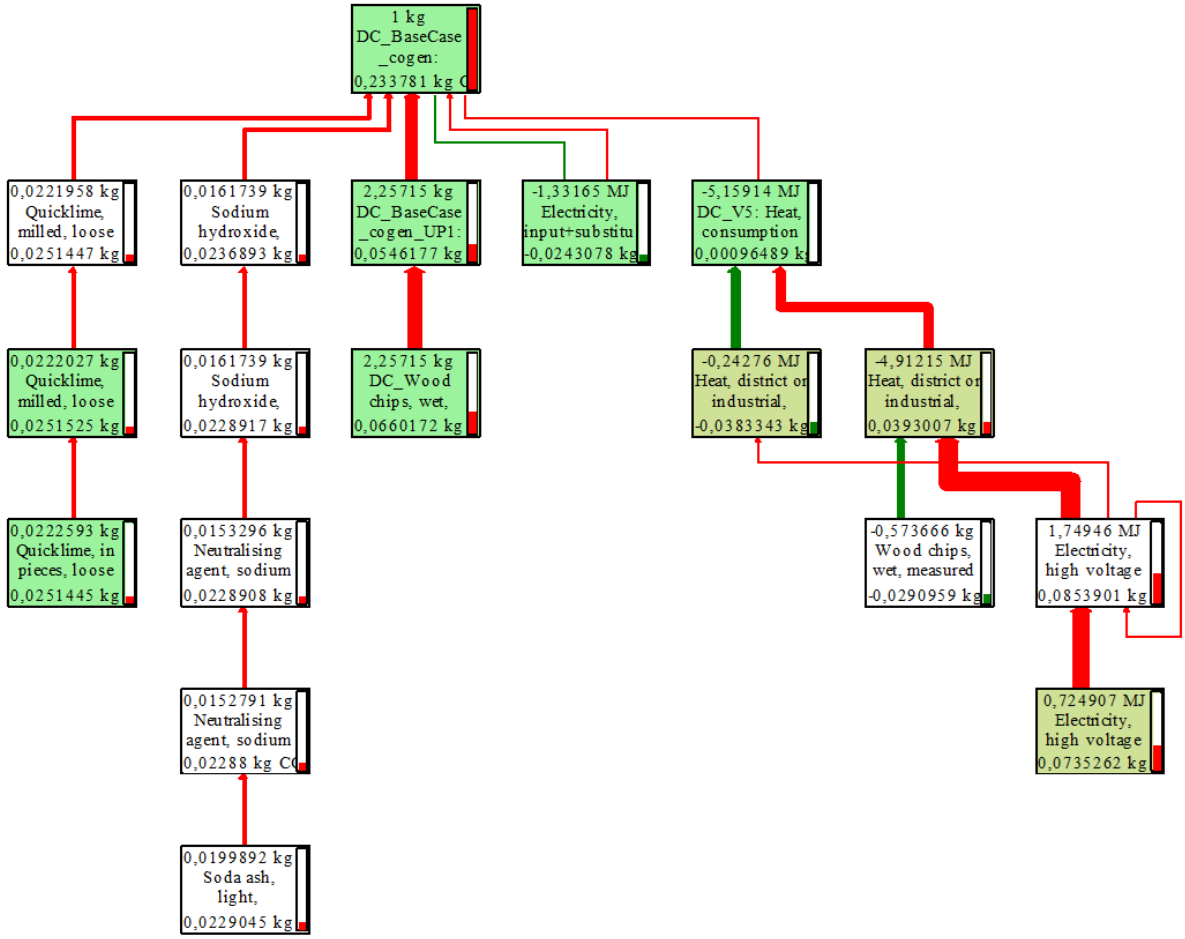

Figure S14. Climate change network for S1-Burn scenario.

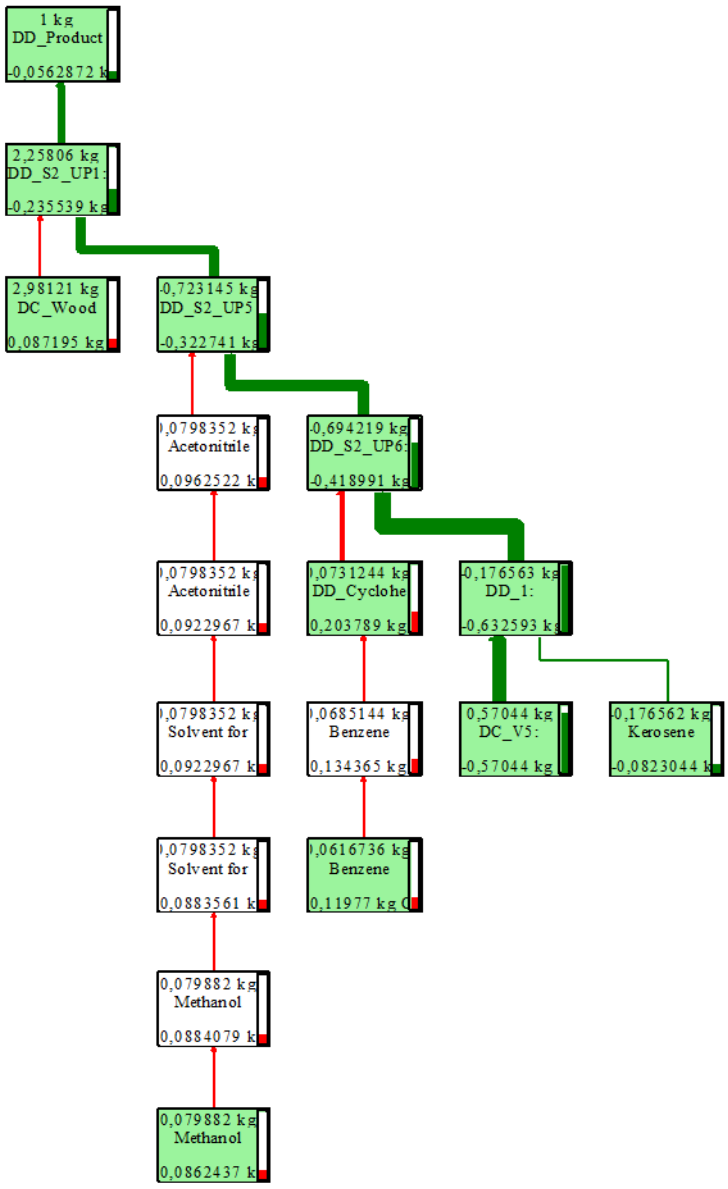

Figure S15. Climate change network for S2-AF scenario.

Carbon balance

Table S18. Carbon balance for the optimized HDO reaction. HDO of cycloadducts was catalysed by Ru/C with HY zeolites (Si/Al ratio of 30) at 220 °C and under the hydrogen pressure of 40 bar. Reaction time was 16 h.

Carbon yield, %							
$C_{10}H_{20}$	C_9H_{18}	C_8H_{16}	C_7H_{14}	C_8-C_{10} oxygenates	C_5H_{12}	THP	Total
9	20	18	10	5	6	-	68

Total carbon yield was calculated for the transformations starting from furfural by multiplying the yields after each step:

Total carbon yield = 0.99 x 0.98 x 0.69 x 0.96 x 0.68 x 100 = 0.43 %

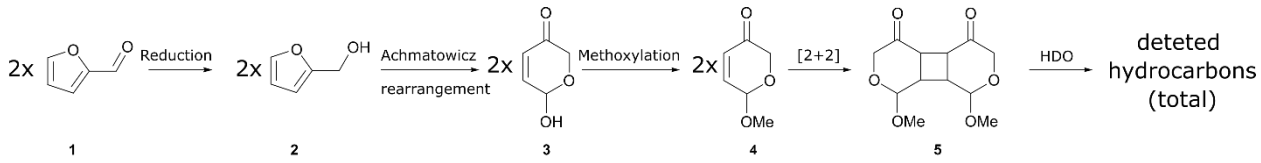

Yield, mol%:	99 mol%	98 mol%	69 mol%	96 mol%	51 mol% (68 carbon%)
Conversion, mol%:	100%	100%	100%	96%	100%

Figure S16. Multi-step transformation of furfural into hydrocarbons. Yields and conversion are given for optimized reaction conditions.

References

1 G. M. Sheldrick, *Acta Cryst A*, 2008, **64**, 112–122.
2 G. M. Sheldrick, *Acta Cryst A*, 2015, **71**, 3–8.
3 A. Marson, J. S. M. Samec and A. Manzardo, *Science of The Total Environment*, 2023, **882**, 163660.
4 L. Zampori and R. Pant, Suggestions for updating the Organisation Environmental Footprint (OEF) method, https://publications.jrc.ec.europa.eu/repository/handle/JRC115960, (accessed February 6, 2024).
5 M. Damiani, T. Sinkko, C. Caldeira, D. Tosches, M. Robuchon and S. Sala, *Environmental Impact Assessment Review*, 2023, **101**, 107134.
6 D. Lebedeva and J. S. M. Samec, *Sustainable Energy Fuels*, 2023, **7**, 3637–3643.
7 L. Shen and M. Patel, *Lenzinger Berichte*.
8 F. F. Furlan, R. T. Filho, F. H. Pinto, C. B. Costa, A. J. Cruz, R. L. Giordano and R. C. Giordano, *Biotechnology for Biofuels*, 2013, **6**, 142.
9 Energimyndigheten, https://www.energimyndigheten.se/, (accessed February 6, 2024).